# Shedding light on aberrant interactions

# Shedding light on aberrant interactions: A review of modern tools for studying protein aggregates

Franziska Kundel[1†], Laura Tosatto[2†], Daniel R. Whiten[1†], David C. Wirthensohn[1†], Mathew H. Horrocks[1,3,†,*], David Klenerman[1,4*]

1. Department of Chemistry, University of Cambridge, Lensfield Road, Cambridge CB2 1EW, UK

2. Centre for Integrative Biology, Università degli Studi di Trento, via Sommarive 9,38123 Trento, Italy

3. Current Address: EaStCHEM School of Chemistry, University of Edinburgh, David Brewster Road, Edinburgh EH9 3FJ, United Kingdom.

4. UK Dementia Research Institute, University of Cambridge, Cambridge CB2 0XY, UK.

†Contributed equally

*Corresponding authors. Email: MHH: mathew.horrocks@ed.ac.uk, DK: dk10012@cam.ac.uk

**Abbreviations:**

| | |
|---|---|
| AD | Alzheimer's disease. |
| AFM | Atomic force microscopy |
| Aβ | Amyloid-beta |
| APP | Amyloid precursor protein |
| αS | α-Synuclein. |
| CD | Circular dichroism |
| Cryo-EM | Cryo-electron microscopy |
| DLS | Dynamic light scattering |
| EMCCD | Electron-multiplying charge-coupled device |
| FCS | Fluorescence correlation spectroscopy |
| FRET | Forster resonance energy transfer |
| FV | Force-volume |
| HC | Healthy controls |
| MAPT | Microtubule-associated protein tau |
| MMP-9 | Matrix-metalloproteinase-9 |

| | |
|---|---|
| NAC | Non-amyloid-β component |
| NFTs | Neurofibrillary tangles |
| PAINT | Point accumulation for imaging in nanoscale topography |
| PALM | Photoactivated localisation microscopy |
| PD | Parkinson's disease. |
| PHF | Paired helical filaments |
| PI3-SH3 | Phosphatidylinositiol-3'-kinase |
| QCM | Quartz crystal microbalance |
| sCMOS | Scientific complementary metal-oxide-semiconductor |
| SF | Straight filaments |
| sPAINT | Spectrally-resolved PAINT |
| STED | Stimulated emission depletion |
| STORM | Stochastic optical reconstruction microscopy |
| TCCD | Two color coincidence detection |
| TCSPC | Time correlated single photon counting |
| TEM | Transmission electron microscopy |
| THS | Thioflavin-S |
| ThT | Thioflavin-T |
| TIRF | Total internal fluorescence |
| uPAINT | Uniform PAINT |

**Abstract:** *The link between protein aggregation and neurodegenerative disease is well established. However, given the heterogeneity of species formed during the aggregation process, it is difficult to delineate details of the molecular events involved in generating pathological aggregates from those producing soluble monomers. As aberrant aggregates are possible pharmacological targets for the treatment of neurodegenerative diseases, the need to observe and characterise soluble oligomers has pushed traditional biophysical techniques to their limits, leading to the development of a plethora of new tools capable of detecting soluble oligomers with high precision and specificity. In this review, we discuss a range of modern biophysical techniques that have been developed to study protein aggregation, and give an overview of how they have been used to understand, in detail, the aberrant aggregation of amyloidogenic proteins associated with the two most common neurodegenerative disorders, Alzheimer's disease and Parkinson's disease.*

## 1. Introduction

Finding an effective therapy for neurodegenerative diseases is one of the most pressing issues in society. The difficulty of this task is partially due to the lack of a precise understanding of the mechanisms underpinning the diseases. Common neurodegenerative

disorders are characterised by progressive neuronal cell loss and the presence of protein aggregates in the affected and surrounding areas of the brain [1–4]. In the context of research into neurodegenerative diseases, the association of these disorders with the aggregation of a specific protein is a relatively recent advance. Whilst the two most common dementias, Alzheimer's disease (AD) and Parkinson's disease (PD) were first described more than a century ago [5] [6], it took more than 75 years to identify the main components of the deposits found in these diseases: in 1985, the peptide amyloid-β (Aβ) was identified as main component of the extracellular plaques found in AD [7] and shortly thereafter neurofibrillary tangles (NFTs) were shown to primarily consist of the microtubule associated protein tau [8–11]. Subsequently, α-synuclein (αS) was identified as main component of Lewy bodies typically present in PD brains [12]. These pivotal discoveries have sparked a vast amount of studies on the role of these proteins on the pathogenesis of AD and PD and other neurodegenerative diseases. However, it has only been more recently that protein aggregation has been studied in great detail on a molecular level.

Whilst the protein deposits found in AD and PD are thought of as archetypical amyloids, protein aggregation has been described as a general property of the polypeptide chain [13,14]. Typically, the aggregation process starts as a consequence of protein misfolding; a protein loses its native conformation and acquires one that is able to self-interact. The process is facilitated in the case of intrinsically disordered proteins, such as Aβ and αS, as their folding energy landscape makes them inherently prone to explore different conformations. Once a nucleus is formed, the aggregates can grow through monomer addition, and further secondary processes can occur to form additional nuclei. For example, secondary nucleation and fibril fragmentation processes have been included in a mathematical model describing protein aggregation to more accurately fit the available data [15–17]. Fragmentation describes the ability of fibrils to break apart and form additional fibrils which can themselves grow and fragment further. Secondary nucleation introduces the possibility that fibrils can recruit monomers to their surface and act as additional nuclei for the growth of other fibrils. Both of these processes may lead to an exponential increase in fibril mass, which may account for disease spreading and progression in the brain.

Although much of our knowledge of protein aggregation has come from *in vitro* studies, fibrils found *in vivo* tend to be morphologically indistinguishable from those formed in the test-tube [18,19]. These *in vitro* studies have made use of recombinant proteins that are incubated under conditions favouring their aggregation, which can vary greatly depending on the protein [20–30]. The resultant aggregation kinetics can then be measured and are usually separated into three main phases: the lag phase, the elongation phase and the final

plateau [31]. These phases are identified as such based on observations made from quantifying protein aggregation using bulk techniques, rather than discrete microscopic steps, and are believed to be shared by all amyloid-forming proteins. The nucleation phase is the name ascribed to the period of time between the initiation of aggregation and the formation of detectable protein aggregates. This phase is the start of amyloid formation, and as mentioned above, necessarily begins with the formation of seeding-competent aggregation nuclei. The elongation phase refers to the period of time where the length of aggregates increases. On the microscopic level, along with continued nucleation, the aggregates grow and associate to form mature amyloid fibrils. The final plateau phase is characterised by the detectable aggregates reaching a dynamic equilibrium with each other and monomeric proteins.

Despite the complications arising from their insolubility and high molecular weights, amyloid fibrils were the first aggregate species described [32]. However, much evidence points towards the earliest species as being the most toxic [33–41]. Unfortunately, these species are highly heterogeneous, rare and transient in nature, and so are difficult to study using traditional biochemical techniques. For this reason, many modern techniques have been developed and adapted to study the aggregates formed in this step of the fibril-formation process. This review describes some of these methods, and goes on to explain how they have led to key findings in the aggregation of the proteins associated with PD and AD, the most common neurodegenerative diseases.

## 2. Overview of techniques

### a) Bulk techniques

#### *Fluorescence*

Historically, the kinetics of *in vitro* fibril-formation have been followed using optical methods. One of the most common techniques makes use of the benzothiazole salt, thioflavin-T (ThT) [42]. Upon binding to β-sheet rich structures, such as amyloid fibrils, the fluorescence quantum yield of ThT increases by several orders of magnitude [43], therefore allowing the quantification of fibril formation (Figure 1a). The dye can be added to time-points taken from an aggregation reaction, and its fluorescence measured in a conventional fluorimeter (*ex situ*). Alternatively, it can be added to a solution of aggregating protein *in situ* and the fluorescence increase can be measured continuously with a plate-reader. However, care must be taken to ensure that the dye itself does not affect the aggregation process. The advantage of this method is that it is simple to implement, requiring inexpensive equipment,

and little training. Much work has also focused on fitting mathematical models to the resultant fluorescence traces to gain insights into the kinetics involved in the fibril-formation process, such as determining the relative contributions of primary nucleation, elongation, secondary nucleation and fragmentation [44–46]. However, such optical techniques only observe the ensemble fluorescence from the system, and so limited information on the individual species contributing to this enhanced fluorescence is obtained. Moreover, not all aggregates bind ThT, meaning some species important to disease pathology may be missed [21]. For this reason, a range of new dyes have been developed, some of which can detect a wider range of aggregates [47,48].

### *Dynamic light scattering (DLS)*

Whereas bulk optical methods enable the total relative β-sheet mass of a sample to be measured over time, other methods offer insights into the actual sizes of the species present. DLS the scattering of laser light by small insoluble particles to gain information on the size distribution of a sample. This method is often used in the study of protein aggregates [49], and allows information to be obtained on the size of the aggregates (Figure 1b). Once again, it has the advantage of being simple to implement and no potentially interfering dye or chemical is required. However, DLS provides the average size of the species present rather than the sizes of the individual aggregates. The technique is also biased towards larger species, which have a greater propensity to scatter light. Additionally, DLS has a practical resolution limit of approximately 1 nm which is imposed by factors such as sample purity and the wavelength of the laser being used.

### *Circular dichroism (CD)*

In addition to the size distribution of aggregating species, the average protein structure can also be measured using techniques such as CD. CD exploits the ability of regular amino acid structures within proteins to rotate the polarisation of light to provide information on the secondary and tertiary structures of proteins. This is useful for studying protein aggregation, since many of the proteins that aggregate are intrinsically disordered in their native state, and so have very little distinct secondary or tertiary structure; however, when forming amyloid structures, the β-sheet content increases, and measuring this can provide structural insights into the fibril formation process (Figure 1c) [50].

b) Surface-based techniques:

*Quartz crystal microbalance*

To overcome some of the shortfalls of ensemble techniques, surface-based methods have also been used to characterise the aggregation process. Quartz crystal microbalance (QCM) sensors are able to determine mass variation per unit area by measuring the change in frequency of a resonating quartz crystal. This method is sensitive enough to report on the change in mass of surface-attached fibrils and has enabled very precise measurements of the influence of solution conditions on αS fibril elongation to be obtained [52].

*Atomic Force Microscopy*

Atomic force microscopy (AFM) enables the surface topography of a sample to be deduced as a cantilever and tip raster scans a surface [53]. A laser beam reflected from the tip is detected by a photodiode detector, enabling the topography of the sample to be mapped with a vertical resolution of less than 1 nm, although the horizontal resolution is lower. These techniques have the advantage of being label-free, and in the case of AFM, allow individual aggregates to be observed. However, they are sensitive to surface effects which may perturb the findings [54]; for example, fibrils may grow at different rates on the surface, and some species may have a greater propensity to adsorb on the surface than others.

c) Fluorescence based single-molecule techniques

The protein aggregation process leads to the generation of a wide range of species, from highly heterogeneous oligomers, through to amyloid fibrils, which have a well-defined structure. For this reason, the ability to characterise individual aggregates using single-molecule fluorescence methodologies has revealed much about protein aggregation. To visualise individual molecules, the signal-to-noise ratio must be high, and one way in which this is achieved is through the reduction in the excitation volume. There are two principal methods by which this is brought about: confocal microscopy and total internal reflection fluorescence (TIRF) microscopy.

*Confocal microscopy techniques*

In single-molecule confocal microscopy, a collimated laser beam is focused by a high numerical aperture objective lens to a diffraction limited spot (< 1 μm). As individual dye-tagged molecules are excited in the confocal volume, their fluorescence emission is

collected by the same objective lens, filtered, and passed through a pinhole (to reject out of focus light) and focused onto a highly sensitive avalanche photodiode detector (Figure 2a). Confocal microscopy was first used in this way to study the aggregation of the SH3 domain of phosphatidylinositiol-3'-kinase (PI3-SH3) [55]. In this study, equimolar mixtures of two different dye-labelled PI3-SH3 solutions were incubated under conditions favouring protein aggregation, and regular samples were collected to be analysed using two color coincidence detection (TCCD). With TCCD, two confocal volumes of different wavelengths are overlapped, in this case 488 nm (blue) and 633 nm (red). As dye-tagged molecules transverse the overlapped volumes, they generate bursts of fluorescence. Monomeric PI3-SH3 only gave rise to a signal in either the blue-excitation, or red-excitation channel, whereas the oligomers generated a coincident signal in both channels if they contained both dyes (Figure 3a). This method therefore provided the means to separate oligomeric events from monomers and the total intensity provided information about the sizes of the oligomers. In a similar technique, scanning for intensely fluorescent targets (SIFT) [56,57], the two overlapped laser beams are scanned through the sample to detect species.

In some cases, the different colour dye molecules in the oligomers formed are close enough for Förster resonance energy transfer (FRET) to occur between them. This allows for the use of one-color excitation (to excite the donor fluorophores), and emission in the acceptor channel denotes the presence of an oligomer (Figure 3b). This has been used to study the aggregation of a variety of proteins as the FRET efficiency can be used to determine the relative mean distance between the fluorophores, giving some insights into the monomer density within an aggregate [35,58,59]. Surface effects are removed in solution-based confocal microscopy; however, data interpretation is more complex, since structures must be inferred from bursts of fluorescence. Additionally, the low concentrations (sub-nanomolar) required for single-molecule confocal measurements may mean that many species dissociate upon dilution, and so are not observed. However, microfluidic devices to rapidly dilute samples before complexes have had the chance to dissociate have been designed, and these could go some way to remedying this potential problem [60].

In contrast to discrete burst analysis, a confocal microscope setup can also be used to perform fluorescence correlation spectroscopy (FCS) [61,62]. FCS relies on measuring temporal fluorescence fluctuations as multiple fluorophores occupy the confocal volume (concentrations of 1-100 nM). The careful analysis of such fluctuations through autocorrelation and fitting to relevant diffusion equations enables the determination of concentrations and diffusion coefficients. However, the method does not strictly observe individual molecules, and deconvolution of multiple populations can be troublesome.

*Total internal reflection fluorescence (TIRF) microscopy techniques*

In contrast to confocal microscopy, TIRF microscopy is usually a surface-based method. Total internal reflection occurs when a plane of light travelling through a transparent medium of a given refractive index is incident upon a dielectric interface with another medium of a lower refractive index at an angle greater than the critical angle. Despite being called total internal reflection, an electromagnetic wave termed the “evanescent wave” penetrates a small distance into the second low refractive index medium, and this decays exponentially away from the interface. In objective-based TIRF microscopy [63], collimated laser light from a high numerical aperture objective lens is reflected from the bottom of a glass coverslip containing aqueous solution, and the evanescent wave is used to excite a wide field typically <200 nm into the sample (Figure 2b). The fluorescence is then collected by the same objective, filtered and focused onto either an electron-multiplying charge-coupled device (EMCCD), or a scientific complementary metal-oxide-semiconductor (sCMOS) camera. TIRF microscopy can be used to directly visualise individual labelled aggregates immobilised on a glass slide, allowing their physical size and structure to be imaged, down to a resolution of around 250 nm (the diffraction limit of visible light). The number of monomers present in an oligomer can be estimated using this method. As individual dye molecules within the oligomers photobleach, there is a stepwise decrease in the total intensity of each individual spot, and these can be counted to determine how many dye molecules were present in the oligomer. This becomes problematic if there are too many dye molecules present, but this can be avoided using sub-stoichiometric labelling [64].

In the above described methods, the protein-of-interest must be labelled with an organic fluorophore; however, this can be challenging, and in some cases may affect the kinetics of protein aggregation, or structures of the fibrils [65]. An alternative method uses dyes such as ThT coupled with TIRF microscopy to detect the protein aggregates. This has the advantage of not needing to have the dyes directly conjugated to the protein, and means that the method can be used to observe oligomers within biofluids such as cerebrospinal fluid [51]. However, the binding mechanism of such dyes is not fully understood. They may not bind to all aggregates, and could also bind other structures unrelated to amyloid.

d) Super-resolution microscopy

The diffraction of light limits optical microscopy to a resolution of around 250 nm. However, super-resolution methods [66–68] have enabled optical imaging at much higher resolutions, allowing structures as small as 5 nm to be characterised [69]. There are two main strategies permitting super-resolution microscopy to be performed. One approach, implemented on a

scanning confocal microscope, termed stimulated emission depletion (STED) microscopy, limits the illumination of the sample to regions smaller than the diffraction limit [68]. The other strategy works by stochastically separating single fluorophores in time to gain resolution in space (stochastic switching and readout), and this can be done by various methods. Stochastic optical reconstruction microscopy (STORM) [67] relies on dyes stochastically photoswitching between dark and fluorescent states, allowing subpopulations to be localised individually. Photoactivated localisation microscopy (PALM) [66] uses photoswitchable fluorescent proteins (usually switched to a longer wavelength through irradiation with ultraviolet light) to separate fluorescence from single emitters in time. Other methods, such as point accumulation for imaging in nanoscale topography (PAINT) [70] and uniform PAINT (uPAINT) [71] rely on fluorescent molecules temporarily binding to surfaces, where they are localised to build up a super-resolved image. In adapted versions of this various methods of achieving transient binding have been described, including using short DNA sequences (DNA-PAINT) [72,73]. Additionally, a technique termed spectrally-resolved PAINT (sPAINT) [74] uses the transient binding of the dye nile red to characterise the surface hydrophobicity of protein aggregates. The emission wavelength of nile red varies depending on the hydrophobicity of its environment, and so by detecting the wavelength in addition to the location of nile red binding events, hydrophobicity can be mapped at the nanoscale.

e) Higher resolution

Although super-resolution techniques can now readily achieve imaging with a resolution of greater than 20 nm, this is sometimes not sufficient to fully characterise the smallest of oligomers. Higher resolution methods are routinely used to determine the structure of protein aggregates. Transmission electron microscopy (TEM) uses a tightly focused beam of electrons to image the specimen as they pass through it, and gives rise to a resolution as high as 0.2 nm. Sample preparation for TEM is complex, and this limits its usefulness for looking at some structures. Notably, the Nobel prize in Chemistry has recently been awarded to the developers of cryo-electron microscopy (cryo-EM) [75,76]. In this technique, the sample does not have to be chemically fixed, but is instead rapidly cooled to cryogenic temperatures, meaning that the protein can be observed in its native state. However, the generation of a three-dimensional structure of proteins from cryo-EM relies on reconstructing images from many different projections, and this is challenging for highly heterogeneous specimens, such as oligomers. Nevertheless, it has been used to characterise the structure of purified kinetically trapped oligomers of αS [77], tau filaments extracted from a human AD

brain sample [78], poly-glutamine expanded huntingtin fibrils from cultured neurons [18], and Aβ fibrils [79].

## 3. Alzheimer's disease and the visualisation of amyloid beta aggregates

The presence of extracellular plaques composed of the Aβ peptide is a pathological hallmark of AD [7]. Aβ is formed and released into the extracellular space through the cleavage of the amyloid precursor protein (APP) [80]. This cleavage can be performed by several proteases such as ADAM 10, BACE 1, α- and γ-secretase, leading to the formation of various N- and C-terminal isoforms of Aβ exist [81,82]. When the expression and degradation of Aβ is controlled there is evidence suggesting that the peptide has several important and possibly neuroprotective functions, such as regulating synapse activity [83]. However, when the homeostatic balance of Aβ production is disturbed the aggregation of the peptide plays a key role in neurodegeneration [84–86]. As a result, much effort has been dedicated to characterising aggregated Aβ species. It is not clear precisely which factors lead to the loss of the normal balance, however the ratio of the most abundant cleavage products Aβ1-40 and Aβ1-42 has been implicated to be important to AD pathogenesis, adding greater complexity to the oligomer formation process [87].

Due to the high aggregation propensity of Aβ, it can be challenging to obtain a homogeneous monomeric sample, as the molarities required for many ensemble methods are high enough to trigger aggregation. This makes studying the kinetics of aggregation troublesome, since there may already be seeds present which can complicate the reaction. Despite this, a variety of soluble aggregates have been studied, but most have not been characterised beyond the use of SDS-PAGE and antibody reactivity[88]. Beyond this, various structural and functional details have been obtained for water-soluble, non-fibrillar Aβ assemblies [88]. Structures that have been described include protofibrils [89,90], Aβ-derived diffusible ligands [91,92], globulomers [93], spheroids [94,95], disulphide cross-linked Aβ [27], cell-derived SDS-stable low n-oligomers [96,97], Aβ*56 [98] and a brain-derived SDS-stable Aβ-dimer [27],[88]. They all have in common distinctly different biological effects compared with mature fibrils, although some of them contain cross β-sheet structures, such as the protofibrils [89,90].

The most commonly used techniques to characterise Aβ aggregates are AFM and TEM. Both techniques are used to examine the morphological differences exhibited by various aggregates, such as elongated amyloid fibrils and small, globular oligomers [99–102]. These approaches have been used to study all species throughout the aggregation process, as

well as comparing the structure of aggregates produced by mutant variants [103,104]. AFM studies showed that not only the morphology of aggregates changed throughout the aggregation process, but the Young's modulus (a measure of stiffness) also increased, suggesting an internal structural rearrangement [105]. Furthermore, Aβ fibrils have been resolved at the atomic level with X-ray crystallography and solid state-NMR including variations in clinical subtypes of AD [106–108]. Structures of the cross β-sheet amyloid state are reviewed in great detail by Eisenberg and Jucker [109]. A complete *de novo* 42 amino acid atomic model of Aβ fibrils has also recently been solved via cryo-EM [110].

Fluorescently labelled Aβ peptide variants are readily available as solid-phase synthesis allows the efficient site-specific conjugation of single fluorescent tags to the Aβ peptides. This has facilitated the use of highly sensitive single-molecule methods to study the properties of individual Aβ aggregates, especially oligomers. The application of single-molecule methods to study early aggregates has provided insights into the size distributions and effects of very early aggregates [111–113]. Narayan and colleagues found that Aβ oligomers initiated neuronal damage on astrocytes [114] and were sequestered by an extracellular chaperone [112]. They described the oligomers as mostly below 10-mers in monomer units, and using TCCD it was possible to study these at levels much closer to their physiological concentrations compared to other techniques [115]. Furthermore, these fluorescent methods have been used to show how oligomers preferentially interact with cell membranes relative to monomers [116]. Subsequently, Flagmeier et al. used an ultrasensitive membrane disruption assay to show that Aβ42 oligomers but not monomers or fibrils are able to disrupt lipid vesicles at picomolar concentrations [86].

Aggregate analysis via TCCD and confocal photobleaching trajectory analysis [117] are limited by acquisition times and instrumental dead times. Whilst the timescale of *in vitro* aggregation of the majority of amyloidogenic proteins is sufficiently slow to take full advantage of these techniques, the temporal resolution can be a limiting factor for the ability to detect early aggregation events of proteins with fast aggregation kinetics, such as Aβ42. To overcome this limitation, microfluidic strategies have been used, whereby the aggregation mixture is rapidly flowed through the confocal volume to increase the rate of detection, and therefore increase the time-resolution of the methods [58].

TCCD measurements of co-oligomer formation between Aβ40 and Aβ42 helped generate a thermodynamic model of the peptides' aggregation propensities [118]. It should be noted that the ability to size aggregates from TCCD and smFRET measurements is limited due to several factors such as the inhomogeneity of the confocal volume and fluorescence quenching at high label densities. Improvements to the former have been suggested by

Murphy *et al.* through the use of Bayesian Inference [119], which led to the data analysis on population sizes and intramolecular distance being more robust than simple threshold-based analysis, especially in more complex datasets.

Super-resolution techniques have been used to probe the seeding capacity of Aβ aggregates in addition to the morphology of aggregates in CSF [120,121]. By seeding fluorescently labelled Aβ40 with brain- and CSF-derived Aβ from AD and control patients it has been shown, using dSTORM, that seeding capacities and elongation rates were dependent on aggregate size [122].

In order to perform label free imaging *in vivo*, there has been a surge in the development of fluorescence imaging probes with similar properties as ThT and Thioflavin S (ThS). Notably the class of oligothiophenes has been used to image Aβ aggregates in their pre-fibrillar and fibrillar state both *in vitro* and *in vivo* (**Error! Reference source not found.**) [123–125]. Interestingly, these dyes show different spectral footprints for the different amyloid topologies of Aβ and tau [126]. Similarly, the hydrophobicity reporter dye nile red has been used to spectrally super-resolve local hydrophobicity propensities of amyloid aggregates using sPAINT [74].

A different approach in understanding the molecular mechanisms of aggregation, and hence oligomer formation, is through the combination of high quality kinetic data and kinetic modelling. This work on Aβ has been pioneered by the Knowles and Linse groups. High purity recombinant monomeric Aβ42 has led to robust aggregation kinetics which has enabled the use of global fitting models to get insight into molecular mechanisms of the underlying processes [127–129].

An online modelling platform has been made available to investigate the effect of interactions of Aβ with, for example chaperones [130] or antibodies [131] and to model molecular mechanisms for other amyloid proteins [128]. This has shown that Aβ42 aggregation is strongly dominated by secondary nucleation, and hence the presence of seeds has an autocatalytic effect on the aggregation process [15]. However, care needs to be taken when inferring *in vivo* mechanisms from *in vitro* models, as some of the effects may be compounded by cellular components, for example fibril seeding on the membrane.

The application of the above mentioned advanced biophysical methods has led to insights into the molecular mechanisms underlying Aβ aggregation, and has given us insights into some structural features of the resulting soluble aggregates and amyloid fibrils. One of the main challenges is to link these molecular mechanisms and structural features to the

resulting neurological effects and finally to the clinical manifestation of the disease. The prolonged time-course of the disease and the low Aβ concentration in the extracellular space are of particular interest. *In vitro,* Aβ aggregation time-courses are usually studied over hours at concentrations that are orders of magnitudes higher of what is found in the CSF [132]. Furthermore, the interactions and interplay between different Aβ peptide isoforms and with other amyloid forming proteins have not been conclusively explored. The application of the techniques to describe here could allow the investigation of these problems at the atomic and molecular level and help understand the neurobiology of these diseases.

## 4. Tau oligomers and filaments

The aggregation of the microtubule associated protein tau into intracellular deposits plays a central role in the pathogenesis of AD and more than 20 other neurodegenerative disorders, collectively termed tauopathies [133]. Six different tau isoforms are produced in the adult human brain by alternative splicing of the MAPT (microtubule-associated protein tau) mRNA [11,134–138]. These have up to two N-terminal inserts and either three or four repeat regions (termed R1-R4) in the C-terminal half [139]. The vast majority of tauopathies are sporadic diseases with age being the main risk factor, however almost 80 pathogenic exonic missense and intronic silent mutations in the tau gene have been found in inherited cases of frontotemporal dementia [140–144]. These mutations tend to cluster around the repeat regions of tau which mediate microtubule binding and play an important role in the aggregation of tau as they form a large part of the core region of tau filaments [145,146]. Intronic mutations and some mutations in exon 10 interfere with the alternative splicing of tau mRNA, increasing the amount of 4 repeat tau over 3 repeat tau. Pathological tau is hyperphosphorylated and contains about 8 moles of phosphate per mole of protein compared to 2-3 moles per mole of protein in physiological tau [147,148].

AFM and TEM have offered some important insights into the aggregation mechanism of tau. Notably, due to their high resolution, these techniques were successfully used to study small oligomeric tau species as well as ultrastructural properties of filamentous tau. Barrantes *et al.* used atomic force microscopy and spectroscopy to study tau aggregation *in vitro* in the absence of any inducers of aggregation. They found that tau rapidly forms heterogeneous granular oligomers with a height of 6-16 nm at room temperature, whereas fibrillar material was detectable only after a few months of incubation. Further, they showed using force spectroscopy that the interaction between tau monomers is relatively strong and required unbinding forces in the order of ligand-receptor or antigen-antibody interactions [149]. The formation of prefibrillar granular tau aggregates of similar size (15-25 nm) was also found in

two further studies, where tau aggregation was induced by the addition of heparin [150,151]. These granular aggregates formed at the end of the lag phase and appeared to be ThT-active, indicating that these species are β-sheet rich aggregates. Interestingly, Maeda *et al.* could isolate such granular tau aggregates from AD patients as early as Braak stage I, before filamentous tau was detectable. The authors therefore suggested that these species represent early tau assemblies preceding mature filaments [150,152].

High resolution AFM and TEM were also used to assess the morphology and mechanical stability of tau fibrils formed in the presence of heparin. The high resolution of these techniques allowed the determination of the thickness and periodicity of tau fibrils and demonstrated their polymorphic nature [153]. In the same study it was also shown that hydrophobic surfaces or mechanical force by the AFM cantilever can lead to the fragmentation of tau fibrils into species with a similar morphology to the granular oligomers described above. This suggests that granular tau species could not only exist as a precursor of filaments but could also be produced by the fragmentation of fibrillar species. This highlights that care must be taken to identify and avoid artefacts when surface-dependent methods are employed to characterise amyloid species. In a second study by Wegmann *et al.*, high resolution AFM was used in force-volume (FV) mode to study the orientation of the N- and C-terminal projection domains of full length tau [154]. FV-AFM is ideal to image biomolecules with high force sensitivity, and to simultaneously map their physicochemical properties at molecular resolution (1-2 nm) [155]. Using FV-AFM, the authors described the projection domains of tau, the “fuzzy coat”, as highly flexible polyelectrolyte brush surrounding the fibrillar core of tau. This coat is around 16 nm thick and mechanically up to four times softer than the fibrillar core [154]. Scanning transmission electron microscopy is able to provide mass per unit length measurements and has shown that tau filaments have a mass per length of 160 kDa (≈3.5 monomers) per nm for recombinant full length tau (2N4R Δ280K tau) and 130 kDa per nm for AD paired helical filaments (PHFs) [156].

Notably, the advent of cryo-EM has recently allowed the first atomically-resolved (3.4-3.5 Å) visualisation and reconstruction of PHFs and straight filaments (SFs) extracted from a patient with AD [146]. This work confirmed that tau filaments are formed of two identical protofilaments with C-shaped subunits and that PHFs and SFs differ in the orientation and packing of these two protofilaments, as previously suggested based on lower resolution electron micrographs[157]. In their work, Fitzpatrick *et al.* provide, for the first time, full atomic maps for the tau filament core in PHFs and SFs (see Figure 5). This core region spans residues 306 to 378 of full length tau, corresponding to the repeat regions R3 and R4 and a short stretch beyond R4 [78].

Similar to Aβ, important mechanistic insights into the aggregation of tau have been gained by kinetic modelling. Whilst tau aggregation has been described by simple nucleation-elongation models [158,159], the *in vitro* aggregation process of tau is complex as inducers of aggregation seem to act as ligands or allosteric regulators which bind transiently to tau [160,159,161–164]. This catalyses a conformational change of tau leading to the rapid formation of small nuclei. The lowered thermodynamic barrier of nucleation results in rapid aggregation kinetics even at very low protein concentrations, and without the presence of the classical lag time, a process which cannot necessarily be assigned to a canonical nucleation-polymerisation model [160]. Using confocal smFRET, Shammas *et al.* were able to track the evolution of transient K18 tau oligomers during aggregation, and demonstrated that the disease associated tau mutations ΔK280 and P301L lead to the formation of around 50-fold more transient oligomers compared to wild-type tau during their aggregation (see Figure 6b) [165]. Similar trends were observed by Kumar *et al.*, who used AFM and time correlated single photon counting (TCSPC) to study the oligomerisation of K18 tau [166]. Further, kinetic analysis of the oligomerisation process revealed that K18 tau aggregation, similar to αS [167], proceeds via monomeric assembly into small oligomers followed by a slow structural conversion step before fibril formation (Figure 6) [165]. Rate constants of the fundamental microscopic reaction steps could be determined, showing that the disease-associated mutants have an increased nucleation rate compared to wild-type tau. As the primary nucleation of wild-type tau is comparatively slow and acts as a bottle-neck for aggregation, the authors predict that small amounts of seeds have a large effect on the amplification of wild-type tau aggregates in cells. In contrast, seeding is thought to play a less significant role for mutant tau with aggregation being dominated by primary nucleation [165]. This hypothesis is in agreement with a previous study in mice showing more efficient propagation of pathology by wild-type tau as compared to mutant tau [168]. Whilst a recent study provided some indirect evidence for secondary processes to occur during the aggregation of the short repeat domain construct K18 tau [169], the aggregation kinetics of full length tau appear not to be dominated by secondary processes such as secondary nucleation or fragmentation [159].

The high sensitivity of smFRET for small oligomeric species has also been exploited to study the interaction of the molecular chaperone Hsp70 with different aggregate species of the K18 ΔK280 tau variant. This study showed that Hsp70 slows down the nucleation process of tau, stabilises oligomeric species and inhibits their growth into fibrils [170]. Similar findings were made in a second study, comparing the action of Hsp70 and a second chaperone, HspB1, on K18 and full length tau aggregation using FCS and NMR [171].

Similar to TCCD and FRET, Giese and co-workers developed a method for the sensitive detection of protein aggregates. Using their technique, referred to as SIFT, the Giese lab identified the trivalent metal ions $Al^{3+}$ and $Fe^{3+}$ and organic solvents, such as dimethyl sulfoxide, as inducers of tau self-oligomerisation and co-aggregation with αS [172]. The latter was found to be moderately enhanced by tau phosphorylation [173]. Furthermore, they used FCS to study the effect of limited proteolysis of tau on its oligomerisation propensity. They showed that limited proteolysis by the extracellular matrix-metalloproteinase-9 (MMP-9) leaves the repeat domain of tau largely intact, leading to the formation of an aggregation-prone fragment of tau [174].

In a number of studies Rhoades and colleagues investigated interactions of tau with pathological and physiological targets. Using FCS, they show that lipid bilayers catalyse the aggregation of K18 tau by serving as a nucleation surface. Once a critical surface density is reached, tau aggregates into ThT-active species incorporating the lipid vesicles [175]. In a second study, Rhoades and co-workers systematically introduced FRET pairs distributed over the whole tau sequence to study its conformation in the absence and presence of an aggregation inducer, heparin [164]. In agreement with a previous bulk study by the Mandelkow lab [176], the N- and C-termini of monomeric tau were found to fold loosely over the microtubule repeat. Upon addition of heparin, tau undergoes a critical conformational change characterised by the loss of these long-range contacts and a contraction of the repeat region [164]. Furthermore, the distance between the different FRET pairs derived in the smFRET experiments described above served as constraints to model the conformational ensemble of tau during aggregation [177] It should be noted that whilst FRET provides valuable conformational information under physiological conditions, conformational artefacts may arise from the covalent attachment of the FRET dyes to the protein of interest.

Another approach making use of organic fluorophores covalently attached to tau was chosen by Kaminski and Kaminski-Schierle. They demonstrated that the fluorescence lifetime of labelled aggregates changes with the appearance of β-sheet containing structures and that this change can be used to assess the aggregation state of amyloidogenic proteins *in vitro* and *in vivo* [178]. In a recent study by Michel *et al.*, this principle was used to track the fate of monomeric K18 tau added to the extracellular medium of SH-SY5Y cells [179]. Importantly, in this study, 10% labelled K18 tau-AF488 and 90% unlabelled protein was used to reduce dye-dependent artefacts. Confocal TCSPC microscopy showed that tau was rapidly taken up into endosomal compartments and formed aggregates which appeared to seed endogenous tau [179]. Furthermore, two colour dSTORM imaging of the cell medium revealed that cells seeded with monomeric tau expelled fibrils into the cell medium

consisting of both endogenous and exogenously added tau. Interestingly, single fibrils contained multiple regions containing exogenous tau ("seed tau") rather than one region comprising the "core seed", which is not compatible with the simple elongation by monomer addition mechanism conventionally assumed for seeded aggregations. Fluorescence lifetime measurements were also used to assess the density of K18 tau fibril clusters as the fluorophores undergo strong self-quenching when in close proximity to each other [180]. Hereby it was also sufficient to have a fraction of the protein labelled with the organic fluorophore, requiring labelling ratios of 10% or higher. Surprisingly, whilst this assay appeared to be very efficient at detecting the formation of fibril clusters, fluorophores in single fibrils were not quenched and thus this method is not suitable to study the early aggregation steps such as the conversion of disordered oligomers to well-ordered fibrils [180]. Whilst the use of partially labelled tau samples, in which only a fraction of tau molecules is fluorescently labelled, leads to a decreased detection efficiency for smaller protein aggregates such as very small oligomeric species, it can be an efficient strategy to reduce the influence of the label on the aggregation behaviour. Generally, this approach can therefore be a good compromise when the amyloidogenic protein of interest is difficult to label in a non-perturbative way and ultrasensitive measurements are not crucial for the study to be conducted.

Notably, for *in vivo* studies direct labelling is not applicable and immunostaining with labelled antibodies is commonly performed. Benda *et al.* demonstrated the use of STED microscopy to image immunostained tau aggregates in 50 µm AD brain sections. They achieved a spatial resolution of 77 nm, allowing the visualisation of single fibrils within NFTs. Also, small tau puncta and fibrillar fragments were observed in close proximity to the tangles. Furthermore, the resolution in the x-y plane could be maintained when z-stacks were recorded over 20 µm, allowing three-dimensional surface rendering of NFTs (although with confocal axial resolution). Ultrastructural features of filaments could not be resolved [181].

In summary, some important insights have been gained into the aggregation pathway of tau by advanced biophysical methods such as TEM and fluorescence microscopy. For tau, remaining challenges are a more comprehensive characterisation of small soluble species of the full length protein *in vitro* and *in vivo*, and the identification of mechanisms of toxicity conferred by such species. This field will benefit from improved labelling strategies, e.g. through more readily available site-specific labelling strategies or the development of nanobodies for tau, and new super-resolution techniques such as DNA-PAINT [73]. Furthermore, the ability to resolve aggregates at the atomic level by cryo-EM [75,76] will allow more profound insights into the ultrastructural features of tau filaments and will provide

important insights into the prion like character of tau, e.g. through the analysis of filaments found in other tauopathies.

## 5. Alpha-synuclein and Parkinson's disease

αS is the major component of Lewy bodies found in PD and in other synucleinopathies [12]. It was one of the first described intrinsically disordered proteins, and has also been associated with amyloid plaques in AD [182]. In addition to its presence in Lewy bodies, the link between αS and PD is also evidenced by the duplication and triplication of the *SNCA* gene encoding αS leading to autosomal dominant forms of the disease [183,184], in addition to single residue missense mutations also causing early-onset forms of PD [185–190].

The primary structure of αS can be divided into three regions: the positively charged N-terminal region (residues 1-60), which contains imperfect repeats that resemble the apolipoprotein helical sequence and drive the acquisition of alpha-helix upon binding to membranes [191,192]; the central hydrophobic domain (residues 61-95), also called NAC (non-amyloid β-component), which is responsible for its aggregation and leads to the formation of beta-sheet during fibril formation [193,194]; and finally, the acidic C-terminal end (residues 96-140), which has a high proportion of negatively charged residues and prolines, contributes to protein solubility and has never been associated with α-helical or β-sheet secondary structure [195]. αS has been described as a chameleon, as it is able to acquire different secondary structures depending on interaction with lipids and other proteins [196].

Despite the large majority of PD cases being sporadic [197], it is interesting to note that all disease-causing mutations are in the same N-terminal region of the protein just prior to the NAC region, indicating that mutations can influence the conformational landscape of αS and modulate its propensity to acquire secondary structure [198]. It has been shown that these mutations can indeed modulate *in vitro* and *in vivo* aggregation properties of αS [29,199–203]. Some mutations are known to increase the aggregation tendency of αS, such as A53T and E46K [199,202,204], while others delay fibril-formation, for example A30P and G51D [29,203]. For the A30P mutation in particular, the hypothesis that αS forms a trapped population of oligomers that cannot go on to form fibrils has led to the belief that oligomers are responsible for inducing toxicity in PD [29]. However, as for other aggregating proteins, direct detection of these highly heterogeneous species has remained challenging. Alongside methods developed for studying other aggregating proteins, a number of techniques for characterising αS aggregates have also been established.

One of the earliest approaches was to find conditions that generate a large amount of oligomers. One such method involved incubating concentrated solutions of αS on ice, leading to the formation of annular oligomers analysed using TEM [205] (see Figure 7). Other protocols involve incubating αS at 37 ºC [206,207] and inserting a size exclusion [208,209] or diafiltration step [210] to generate adequate amounts of oligomers for further studies. One such study [207] purified a kinetically-trapped oligomeric species that was accurately characterised using fluorescence, CD, AFM, DLS and cryo-EM. However, many types of such oligomers often do not proceed to form fibrils, but are instead trapped in an energy well for alternative aggregation/folding of αS, and so may not represent the real heterogeneity of αS oligomers [208,211–213]. However, this is not always the case, and in other cases, purified oligomers are able to go on to form fibrils [214,215]. Additionally, the type of oligomers formed is strongly dependent on the experimental conditions used [216]. Several additives have been used to boost the formation of these aggregates. Dopamine and fatty acids are often used to stabilise oligomers [211,215,217–221]. Oligomers obtained with these techniques have β-sheet content, in some cases α-helical content, are stable upon shifts in pH and temperature [222] and can interact with lipid membranes and cells [206,214,222–225]. These and other conditions have been extensively reviewed recently [226].

To the best of our knowledge, αS oligomers obtained from brain extracts have not been structurally characterised, meaning that there is no possibility to compare these oligomers with the ones formed *in vitro*. The end point of aggregation *in vivo* are amyloid fibrils, which are similar to those formed *in vitro* [18,19], thus suggesting that similar intermediate species may be formed throughout the processes. In an attempt to characterise some of the most elusive species, cross-linking techniques have been applied to capture the transient oligomers *in vitro* [227,228]. The resultant aggregates have been characterised in terms of their sizes, through use of DLS and SDS-PAGE gels; however, these cross-linked oligomers do not readily form fibrils, as their polypeptide chains cannot adapt or recruit further monomers for elongation [227]. Thus, it is not clear how well these findings represent native oligomers formed within the brain.

Native mass spectrometry has also been used to investigate the sizes of αS oligomers [229]. However, this approach requires the oligomers to be dissolved in specific buffers, which may perturb their structures [230–232]. Data obtained from mass spectrometry describe the presence of different conformational states of monomer, and can detect the formation of dimers [230]. Moreover, drift-time analysis has been used to gain insights into oligomer

topology. Oligomers ranging in size from dimers to hexamers have been described [231]; however, larger oligomers cannot be analysed using such a method.

As for Aβ and tau, fluorescence methods have successfully been employed for the sensitive and specific detection of intermolecular interactions. Structure-based non-covalent fluorescent probes have been developed to specifically detect the presence of oligomers, or pre-fibrillar species during aggregation [233,234]. Alternatively, fluorophores have been conjugated to specific sites of αS using maleimide chemistry on cysteine residues inserted by site-specific mutagenesis on the αS polypeptide chain [177,235,236]. These studies use properties such as pyrene excimer formation to be able to detect intermolecular contacts between αS monomer units. The presence of fluorescent probes on αS also allow FCS measurements to be performed, which enable estimation of size distributions of oligomers from their diffusion coefficients [177]. As is the case for tau, the labelling site for the fluorophores needs to be selected with care: it is important to ensure that the label does not introduce artefacts or affect oligomer formation.

One of the first single-molecule fluorescence techniques applied to studying the aggregation of αS was SIFT [237–240]. As mentioned above, this method looks at the intensities of individual molecules and assigns the brighter bursts of fluorescence as originating from oligomeric species. Furthermore, photobleach step analysis allowed the determination of oligomer sizes in sub-stoichiometrically labelled αS. For this analysis a TIRF setup was used to detect single aggregates rather than a confocal setup as described for Aβ above [64]. The accurate counting of photobleaching steps is usually limited to there being less than ten fluorophores present; in any case, a purified oligomer containing 31 monomer units was identified. However, this method is biased for the detection of brighter species. Additionally, the analysis assumed only one size of oligomer, which may not have been the case.

Through the introduction of a cysteine in the αS sequence at position 90, which is at the edge of the fibril-forming region, detailed analyses on the oligomer formation process have been achieved using the singe-molecule fluorescence methods TCCD and smFRET [35,59,241]. These experiments revealed the existence of two oligomeric populations, with different “compactness”, resistance to proteinase-K degradation and stability in low ionic strength buffers [58]. Furthermore, these techniques enabled a structural comparison of pathologically related mutants in solution, revealing subtle differences structural differences between the oligomers generated by mutants in comparison with the wild type protein [59,242]. The application of this method to aggregation kinetics run at different concentrations of αS permitted the inference of a kinetic model for αS oligomer formation *in*

*vitro*, enabling the calculation of conversion rates between the two different types of oligomers [243].

Unlabelled aggregates of αS have been directly observed using ThT and TIRF microscopy. This technique, referred to as Single Aggregate Visualisation by Enhancement (SAVE) imaging [51], has negated the need for a conjugated organic fluorophore, and so has enabled oligomers to be studied within biofluids. This has led to the finding that cerebrospinal fluid from PD patients contains a greater oligomer load than those samples from healthy controls (HC) (Figure 8). Additionally, sPAINT [74] has been used to look at both oligomers and fibrils of αS, and it was shown that the oligomers have a higher surface hydrophobicity than the fibrils, which may explain their greater toxicity.

Despite the ability to observe oligomers in human biofluids, techniques still need to be developed and adjusted to observe native oligomers in cells or *in vivo*. Due to the low concentration and low stability of these species, oligomer visualisation within cells is challenging, and purification may affect their structure. So far, the large majority of detection methods for proteins *in vivo* is based on the use of antibodies [244,245]. A good number of techniques have been applied to detect αS self-interaction using complementation assays or proximity ligations assays [246–250] or confocal microscopy methods [251,252].

## 6. Conclusion

The rapid development of biophysical methods in the previous decades has clearly led to a greater understanding of some of the molecular processes in neurodegeneration. In particular, these studies were prevalent for proteins available in high amounts through synthetic or recombinant protein production. Both details on the atomic structures of amyloid fibrils, as well as their behaviour within cellular models have been revealed by these methods. Additionally, the kinetics of protein aggregation are now well understood, both in terms of the microscopic processes involved, and which of these dominate for the various proteins. These details enable the rapid assessment of inhibitory factors, and such methods may serve future roles as diagnostic tools, which are vitally needed if a therapeutic strategy is to be developed for neurodegenerative diseases.

Despite the clear advantages of many advanced biophysical methods, their application requires specialist training and equipment and this significant investment of resources places a practical limit on the widespread use of these techniques. The development of new techniques and the ongoing improvement of existing techniques towards faster acquisition times and higher quality data output will allow the application of the techniques to a broader

range of problems. At the same time, biophysical studies need to become more comprehensive, for example by looking for common properties across different amyloidogenic proteins, but also through the use of more biologically relevant samples such as animal model or human post-mortem tissues. Both of these considerations call for a tighter collaboration between different labs in order to make pivotal advances in understanding neurodegenerative diseases. Taken together, the continuous improvement of existing biophysical tools such as super-resolution microscopy and the development of new techniques such as cryo-EM, as well as the improved access to a wide range of different samples, will yield new insights into the pathogenesis of neurodegenerative diseases and will pave the way for future therapies.

**Acknowledgements:**

The authors wish to acknowledge the Royal Society (D.K.), the European Research Council with an ERC Advanced Grant (669237) (D.R.W, F.K., and D.K.). LT is supported by Fondazione Umberto Veronesi Post Doctoral Fellowship 2017. M.H.H. is supported by a Junior Research Fellowship at Christ's College, University of Cambridge, the Herchel Smith Foundation, and the Allen Distinguished Investigator Program, through The Paul G. Allen Frontiers Group.

## References

1 Duyckaerts C (2013) Neurodegenerative lesions: seeding and spreading. *Rev. Neurol. (Paris)* **169**, 825–833.

2 Goedert M, Spillantini MG, Del Tredici K & Braak H (2013) 100 years of Lewy pathology. *Nat. Rev. Neurol.* **9**, 13–24.

3 Goedert M, Ghetti B & Spillantini MG (2012) Frontotemporal dementia: implications for understanding Alzheimer disease. *Cold Spring Harb. Perspect. Med.* **2**, a006254.

4 Chiti F & Dobson CM (2006) Protein Misfolding, Functional Amyloid, and Human Disease. *Annu. Rev. Biochem.* **75**, 333–366.

5 Parkinson J (2002) An essay on the shaking palsy. 1817. *J. Neuropsychiatry Clin. Neurosci.* **14**, 223–236; discussion 222.

6 Alzheimer A (1907) Über eine eigenartige Erkrankung der Hirnrinde. *Allgemeine Zeitschrift fur Psychiatrie und Psychisch-gerichtliche Medizin* **64**, 146–8.

7 Masters CL, Simms G, Weinman NA, Multhaup G, McDonald BL & Beyreuther K (1985) Amyloid plaque core protein in Alzheimer disease and Down syndrome. *Proc. Natl. Acad. Sci. U. S. A.* **82**, 4245–4249.

8 Brion JP, Couck AM, Passareiro E & Flament-Durand J (1985) Neurofibrillary tangles of Alzheimer's disease: an immunohistochemical study. *J. Submicrosc. Cytol.* **17**, 89–96.

9 Grundke-Iqbal I, Iqbal K, Quinlan M, Tung YC, Zaidi MS & Wisniewski HM (1986) Microtubule-associated protein tau. A component of Alzheimer paired helical filaments. *J. Biol. Chem.* **261**, 6084–6089.

10 Pollock NJ, Mirra SS, Binder LI, Hansen LA & Wood JG (1986) Filamentous aggregates in Pick's disease, progressive supranuclear palsy, and Alzheimer's disease share antigenic determinants with microtubule-associated protein, tau. *Lancet Lond. Engl.* **2**, 1211.

11 Goedert M, Wischik CM, Crowther RA, Walker JE & Klug A (1988) Cloning and sequencing of the cDNA encoding a core protein of the paired helical filament of Alzheimer disease: identification as the microtubule-associated protein tau. *Proc. Natl. Acad. Sci. U. S. A.* **85**, 4051–4055.

12 Spillantini MG, Schmidt ML, Lee VM, Trojanowski JQ, Jakes R & Goedert M (1997) Alpha-synuclein in Lewy bodies. *Nature* **388**, 839–840.

13 Chiti F, Stefani M, Taddei N, Ramponi G & Dobson CM (2003) Rationalization of the effects of mutations on peptide and protein aggregation rates. *Nature* **424**, 805–808.

14 Dobson CM (2003) Protein folding and misfolding. *Nature* **426**, 884–890.

15 Cohen SIA, Linse S, Luheshi LM, Hellstrand E, White DA, Rajah L, Otzen DE, Vendruscolo M, Dobson CM & Knowles TPJ (2013) Proliferation of amyloid-β42 aggregates occurs through a secondary nucleation mechanism. *Proc. Natl. Acad. Sci. U. S. A.* **110**, 9758–9763.

16 Buell AK, Galvagnion C, Gaspar R, Sparr E, Vendruscolo M, Knowles TPJ, Linse S & Dobson CM (2014) Solution conditions determine the relative importance of nucleation and growth processes in α-synuclein aggregation. *Proc. Natl. Acad. Sci. U. S. A.* **111**, 7671–7676.

17 Linse S (2017) Monomer-dependent secondary nucleation in amyloid formation. *Biophys. Rev.*

18 Bäuerlein FJB, Saha I, Mishra A, Kalemanov M, Martínez-Sánchez A, Klein R, Dudanova I, Hipp MS, Hartl FU, Baumeister W & Fernández-Busnadiego R (2017) In Situ Architecture and Cellular Interactions of PolyQ Inclusions. *Cell* **171**, 179–187.e10.

19 Conway KA, Harper JD & Lansbury PT Jr (2000) Fibrils formed in vitro from alpha-synuclein and two mutant forms linked to Parkinson's disease are typical amyloid. *Biochemistry (Mosc.)* **39**, 2552–2563.

20 Tomic JL, Pensalfini A, Head E & Glabe CG (2009) Soluble fibrillar oligomer levels are elevated in Alzheimer's disease brain and correlate with cognitive dysfunction. *Neurobiol. Dis.* **35**, 352–358.

21 Lasagna-Reeves CA, Castillo-Carranza DL, Guerrero-Muoz MJ, Jackson GR & Kayed R (2010) Preparation and characterization of neurotoxic tau oligomers. *Biochemistry (Mosc.)* **49**, 10039–10041.

22 Lasagna-Reeves CA, Castillo-Carranza DL, Sengupta U, Clos AL, Jackson GR & Kayed R (2011) Tau oligomers impair memory and induce synaptic and mitochondrial dysfunction in wild-type mice. *Mol. Neurodegener.* **6**, 39.

23 Flach K, Hilbrich I, Schiffmann A, Gärtner U, Krüger M, Leonhardt M, Waschipky H, Wick L, Arendt T & Holzer M (2012) Tau oligomers impair artificial membrane integrity and cellular viability. *J. Biol. Chem.* **287**, 43223–43233.

24 Koffie RM, Meyer-Luehmann M, Hashimoto T, Adams KW, Mielke ML, Garcia-Alloza M, Micheva KD, Smith SJ, Kim ML, Lee VM, Hyman BT & Spires-Jones TL (2009) Oligomeric amyloid beta associates with postsynaptic densities and correlates with excitatory synapse loss near senile plaques. *Proc. Natl. Acad. Sci. U. S. A.* **106**, 4012–4017.

25 Lambert MP, Barlow AK, Chromy BA, Edwards C, Freed R, Liosatos M, Morgan TE, Rozovsky I, Trommer B, Viola KL, Wals P, Zhang C, Finch CE, Krafft GA & Klein WL (1998) Diffusible, nonfibrillar ligands derived from Abeta1-42 are potent central nervous system neurotoxins. *Proc. Natl. Acad. Sci. U. S. A.* **95**, 6448–6453.

26 Li S, Hong S, Shepardson NE, Walsh DM, Shankar GM & Selkoe D (2009) Soluble oligomers of amyloid Beta protein facilitate hippocampal long-term depression by disrupting neuronal glutamate uptake. *Neuron* **62**, 788–801.

27 Shankar GM, Li S, Mehta TH, Garcia-Munoz A, Shepardson NE, Smith I, Brett FM, Farrell MA, Rowan MJ, Lemere CA, Regan CM, Walsh DM, Sabatini BL & Selkoe DJ (2008) Amyloid-β protein dimers isolated directly from Alzheimer's brains impair synaptic plasticity and memory. *Nat. Med.* **14**, 837–842.

28 Ahn M, Hagan CL, Bernardo-Gancedo A, De Genst E, Newby FN, Christodoulou J, Dhulesia A, Dumoulin M, Robinson CV, Dobson CM & Kumita JR (2016) The Significance of the Location of Mutations for the Native-State Dynamics of Human Lysozyme. *Biophys. J.* **111**, 2358–2367.

29 Conway KA, Lee SJ, Rochet JC, Ding TT, Williamson RE & Lansbury PT (2000) Acceleration of oligomerization, not fibrillization, is a shared property of both alpha-synuclein mutations linked to early-onset Parkinson's disease: implications for pathogenesis and therapy. *Proc. Natl. Acad. Sci. U. S. A.* **97**, 571–576.

30 Uversky VN, Li J & Fink AL (2001) Evidence for a partially folded intermediate in alpha-synuclein fibril formation. *J. Biol. Chem.* **276**, 10737–10744.

31 Arosio P, Knowles TPJ & Linse S (2015) On the lag phase in amyloid fibril formation. *Phys. Chem. Chem. Phys. PCCP* **17**, 7606–7618.

32 Shirahama T & Cohen AS (1965) Structure of amyloid fibrils after negative staining and high-resolution electron microscopy. *Nature* **206**, 737–738.

33 Winner B, Jappelli R, Maji SK, Desplats PA, Boyer L, Aigner S, Hetzer C, Loher T, Vilar M, Campioni S, Tzitzilonis C, Soragni A, Jessberger S, Mira H, Consiglio A, Pham E, Masliah E, Gage FH & Riek R (2011) In vivo demonstration that alpha-synuclein oligomers are toxic. *Proc. Natl. Acad. Sci. U. S. A.* **108**, 4194–4199.

34 Rockenstein E, Nuber S, Overk CR, Ubhi K, Mante M, Patrick C, Adame A, Trejo-Morales M, Gerez J, Picotti P, Jensen PH, Campioni S, Riek R, Winkler J, Gage FH, Winner B & Masliah E (2014) Accumulation of oligomer-prone α-synuclein exacerbates synaptic and neuronal degeneration in vivo. *Brain* **137**, 1496–1513.

35 Cremades N, Cohen SIA, Deas E, Abramov AY, Chen AY, Orte A, Sandal M, Clarke RW, Dunne P, Aprile FA, Bertoncini CW, Wood NW, Knowles TPJ, Dobson CM & Klenerman D (2012) Direct Observation of the Interconversion of Normal and Toxic Forms of α-Synuclein. *Cell* **149**, 1048–1059.

36 Outeiro TF, Putcha P, Tetzlaff JE, Spoelgen R, Koker M, Carvalho F, Hyman BT & McLean PJ (2008) Formation of toxic oligomeric alpha-synuclein species in living cells. *PloS One* **3**, e1867.

37 Karpinar DP, Balija MBG, Kügler S, Opazo F, Rezaei-Ghaleh N, Wender N, Kim H-Y, Taschenberger G, Falkenburger BH, Heise H, Kumar A, Riedel D, Fichtner L, Voigt A, Braus GH, Giller K, Becker S, Herzig A, Baldus M, Jäckle H, Eimer S, Schulz JB, Griesinger C & Zweckstetter M (2009) Pre-fibrillar alpha-synuclein variants with impaired beta-structure increase neurotoxicity in Parkinson's disease models. *EMBO J.* **28**, 3256–3268.

38 Luth ES, Stavrovskaya IG, Bartels T, Kristal BS & Selkoe DJ (2014) Soluble, prefibrillar α-synuclein oligomers promote complex I-dependent, Ca2+-induced mitochondrial dysfunction. *J. Biol. Chem.* **289**, 21490–21507.

39 Fagerqvist T, Näsström T, Ihse E, Lindström V, Sahlin C, Tucker SMF, Kasaryan A, Karlsson M, Nikolajeff F, Schell H, Outeiro TF, Kahle PJ, Lannfelt L, Ingelsson M & Bergström J (2013) Off-pathway α-synuclein oligomers seem to alter α-synuclein turnover in a cell model but lack seeding capability in vivo. *Amyloid Int. J. Exp. Clin. Investig. Off. J. Int. Soc. Amyloidosis* **20**, 233–244.

40 Martin ZS, Neugebauer V, Dineley KT, Kayed R, Zhang W, Reese LC & Taglialatela G (2012) α-Synuclein oligomers oppose long-term potentiation and impair memory through a calcineurin-dependent mechanism: relevance to human synucleopathic diseases. *J. Neurochem.* **120**, 440–452.

41 Kaufmann TJ, Harrison PM, Richardson MJE, Pinheiro TJT & Wall MJ (2016) Intracellular soluble α-synuclein oligomers reduce pyramidal cell excitability. *J. Physiol.* **594**, 2751–2772.

42 LeVine H (1993) Thioflavine T interaction with synthetic Alzheimer's disease beta-amyloid peptides: detection of amyloid aggregation in solution. *Protein Sci. Publ. Protein Soc.* **2**, 404–410.

43 Sulatskaya AI, Maskevich AA, Kuznetsova IM, Uversky VN & Turoverov KK (2010) Fluorescence Quantum Yield of Thioflavin T in Rigid Isotropic Solution and Incorporated into the Amyloid Fibrils. *PLOS ONE* **5**, e15385.

44 Knowles TPJ, Waudby CA, Devlin GL, Cohen SIA, Aguzzi A, Vendruscolo M, Terentjev EM, Welland ME & Dobson CM (2009) An analytical solution to the kinetics of breakable filament assembly. *Science* **326**, 1533–1537.

45 Cohen SIA, Vendruscolo M, Dobson CM & Knowles TPJ (2012) From Macroscopic Measurements to Microscopic Mechanisms of Protein Aggregation. *J. Mol. Biol.* **421**, 160–171.

46 Naiki H, Higuchi K, Nakakuki K & Takeda T (1991) Kinetic analysis of amyloid fibril polymerization in vitro. *Lab. Investig. J. Tech. Methods Pathol.* **65**, 104–110.

47 Brelstaff J, Spillantini MG & Tolkovsky AM (2015) pFTAA: a high affinity oligothiophene probe that detects filamentous tau in vivo and in cultured neurons. *Neural Regen. Res.* **10**, 1746–1747.

48 Tong H, Hong Y, Dong Y, Häußler M, Y. Lam JW, Li Z, Guo Z, Guo Z & Zhong Tang B (2006) Fluorescent "light-up" bioprobes based on tetraphenylethylene derivatives with aggregation-induced emission characteristics. *Chem. Commun.* **0**, 3705–3707.

49 Li Y, Lubchenko V & Vekilov PG (2011) The use of dynamic light scattering and Brownian microscopy to characterize protein aggregation. *Rev. Sci. Instrum.* **82**, 053106.

50 Juszczyk P, Kołodziejczyk AS & Grzonka Z (2005) Circular dichroism and aggregation studies of amyloid beta (11-8) fragment and its variants. *Acta Biochim. Pol.* **52**, 425–431.

51 Horrocks MH, Lee SF, Gandhi S, Magdalinou NK, Chen SW, Devine MJ, Tosatto L, Kjaergaard M, Beckwith JS, Zetterberg H, Iljina M, Cremades N, Dobson CM, Wood NW & Klenerman D (2016) Single-Molecule Imaging of Individual Amyloid Protein Aggregates in Human Biofluids. *ACS Chem. Neurosci.* **7**, 399–406.

52 White DA, Buell AK, Knowles TPJ, Welland ME & Dobson CM (2010) Protein Aggregation in Crowded Environments. *J. Am. Chem. Soc.* **132**, 5170–5175.

53 Hansma PK, Elings VB, Marti O & Bracker CE (1988) Scanning tunneling microscopy and atomic force microscopy: application to biology and technology. *Science* **242**, 209–216.

54 Canale C, Torre B, Ricci D & Braga PC (2011) Recognizing and Avoiding Artifacts in Atomic Force Microscopy Imaging. In *Atomic Force Microscopy in Biomedical Research* pp. 31–43. Humana Press.

55 Orte A, Birkett NR, Clarke RW, Devlin GL, Dobson CM & Klenerman D (2008) Direct characterization of amyloidogenic oligomers by single-molecule fluorescence. *Proc. Natl. Acad. Sci.* **105**, 14424–14429.

56 Bieschke J, Giese A, Schulz-Schaeffer W, Zerr I, Poser S, Eigen M & Kretzschmar H (2000) Ultrasensitive detection of pathological prion protein aggregates by dual-color scanning for intensely fluorescent targets. *Proc. Natl. Acad. Sci. U. S. A.* **97**, 5468–5473.

57 Giese A, Bader B, Bieschke J, Schaffar G, Odoy S, Kahle PJ, Haass C & Kretzschmar H (2005) Single particle detection and characterization of synuclein co-aggregation. *Biochem. Biophys. Res. Commun.* **333**, 1202–1210.

58 Horrocks MH, Tosatto L, Dear AJ, Garcia GA, Iljina M, Cremades N, Dalla Serra M, Knowles TPJ, Dobson CM & Klenerman D (2015) Fast Flow Microfluidics and Single-Molecule Fluorescence for the Rapid Characterization of α-Synuclein Oligomers. *Anal. Chem.* **87**, 8818–8826.

59 Tosatto L, Horrocks MH, Dear AJ, Knowles TPJ, Dalla Serra M, Cremades N, Dobson CM & Klenerman D (2015) Single-molecule FRET studies on alpha-synuclein oligomerization of Parkinson's disease genetically related mutants. *Sci. Rep.* **5**, 16696.

60 Horrocks MH, Rajah L, Jönsson P, Kjaergaard M, Vendruscolo M, Knowles TPJ & Klenerman D (2013) Single-Molecule Measurements of Transient Biomolecular Complexes through Microfluidic Dilution. *Anal. Chem.* **85**, 6855–6859.

61 Haustein E & Schwille P (2004) Single-molecule spectroscopic methods. *Curr. Opin. Struct. Biol.* **14**, 531–540.

62 Magde D, Elson E & Webb WW (1972) Thermodynamic Fluctuations in a Reacting System\char22{}Measurement by Fluorescence Correlation Spectroscopy. *Phys. Rev. Lett.* **29**, 705–708.

63 Axelrod D (1981) Cell-substrate contacts illuminated by total internal reflection fluorescence. *J. Cell Biol.* **89**, 141–145.

64 Zijlstra N, Blum C, Segers-Nolten IMJ, Claessens MMAE & Subramaniam V (2012) Molecular composition of sub-stoichiometrically labeled α-synuclein oligomers determined by single-molecule photobleaching. *Angew. Chem. Int. Ed Engl.* **51**, 8821–8824.

65 Anderson VL & Webb WW (2011) Transmission electron microscopy characterization of fluorescently labelled amyloid β 1-40 and α-synuclein aggregates. *BMC Biotechnol.* **11**, 125.

66 Betzig E, Patterson GH, Sougrat R, Lindwasser OW, Olenych S, Bonifacino JS, Davidson MW, Lippincott-Schwartz J & Hess HF (2006) Imaging Intracellular Fluorescent Proteins at Nanometer Resolution. *Science* **313**, 1642–1645.

67 Rust MJ, Bates M & Zhuang X (2006) Sub-diffraction-limit imaging by stochastic optical reconstruction microscopy (STORM). *Nat. Methods* **3**, 793–795.

68 Hell SW & Wichmann J (1994) Breaking the diffraction resolution limit by stimulated emission: stimulated-emission-depletion fluorescence microscopy. *Opt. Lett.* **19**, 780–782.

69 Szymborska A, de Marco A, Daigle N, Cordes VC, Briggs JAG & Ellenberg J (2013) Nuclear pore scaffold structure analyzed by super-resolution microscopy and particle averaging. *Science* **341**, 655–658.

70 Sharonov A & Hochstrasser RM (2006) Wide-field subdiffraction imaging by accumulated binding of diffusing probes. *Proc. Natl. Acad. Sci.* **103**, 18911–18916.

71 Giannone G, Hosy E, Levet F, Constals A, Schulze K, Sobolevsky AI, Rosconi MP, Gouaux E, Tampé R, Choquet D & Cognet L (2010) Dynamic superresolution imaging of endogenous proteins on living cells at ultra-high density. *Biophys. J.* **99**, 1303–1310.

72 Jungmann R, Steinhauer C, Scheible M, Kuzyk A, Tinnefeld P & Simmel FC (2010) Single-Molecule Kinetics and Super-Resolution Microscopy by Fluorescence Imaging of Transient Binding on DNA Origami. *Nano Lett.* **10**, 4756–4761.

73 Jungmann R, Avendaño MS, Woehrstein JB, Dai M, Shih WM & Yin P (2014) Multiplexed 3D cellular super-resolution imaging with DNA-PAINT and Exchange-PAINT. *Nat. Methods* **11**, 313–318.

74 Bongiovanni MN, Godet J, Horrocks MH, Tosatto L, Carr AR, Wirthensohn DC, Ranasinghe RT, Lee J-E, Ponjavic A, Fritz JV, Dobson CM, Klenerman D & Lee SF (2016) Multi-dimensional super-resolution imaging enables surface hydrophobicity mapping. *Nat. Commun.* **7**, ncomms13544.

75 Henderson R & Unwin PN (1975) Three-dimensional model of purple membrane obtained by electron microscopy. *Nature* **257**, 28–32.

76 Henderson R, Baldwin JM, Ceska TA, Zemlin F, Beckmann E & Downing KH (1990) Model for the structure of bacteriorhodopsin based on high-resolution electron cryo-microscopy. *J. Mol. Biol.* **213**, 899–929.

77 Chen SW, Drakulic S, Deas E, Ouberai M, Aprile FA, Arranz R, Ness S, Roodveldt C, Guilliams T, De-Genst EJ, Klenerman D, Wood NW, Knowles TPJ, Alfonso C, Rivas G, Abramov AY, Valpuesta JM, Dobson CM & Cremades N (2015) Structural characterization of toxic oligomers that are kinetically trapped during α-synuclein fibril formation. *Proc. Natl. Acad. Sci. U. S. A.* **112**, E1994–2003.

78 Fitzpatrick AWP, Falcon B, He S, Murzin AG, Murshudov G, Garringer HJ, Crowther RA, Ghetti B, Goedert M & Scheres SHW (2017) Cryo-EM structures of tau filaments from Alzheimer's disease. *Nature* **547**, 185–190.

79 Schmidt M, Rohou A, Lasker K, Yadav JK, Schiene-Fischer C, Fändrich M & Grigorieff N (2015) Peptide dimer structure in an Aβ(1–42) fibril visualized with cryo-EM. *Proc. Natl. Acad. Sci.* **112**, 11858–11863.

80 Haass C & Selkoe DJ (2007) Soluble protein oligomers in neurodegeneration: lessons from the Alzheimer's amyloid β-peptide. *Nat. Rev. Mol. Cell Biol.* **8**, 101–112.

81 Selkoe DJ (1998) The cell biology of beta-amyloid precursor protein and presenilin in Alzheimer's disease. *Trends Cell Biol.* **8**, 447–53.

82 O'Brien RJ & Wong PC (2011) Amyloid precursor protein processing and Alzheimer's disease. *Annu. Rev. Neurosci.* **34**, 185–204.

83 Pearson HA & Peers C (2006) Physiological roles for amyloid β peptides. *J. Physiol.* **575**, 5–10.

84 Sakono M & Zako T (2010) Amyloid oligomers: formation and toxicity of Abeta oligomers. *FEBS J.* **277**, 1348–1358.

85 Santos AN, Ewers M, Minthon L, Simm A, Silber R-E, Blennow K, Prvulovic D, Hansson O & Hampel H (2012) Amyloid-β oligomers in cerebrospinal fluid are associated with cognitive decline in patients with Alzheimer's disease. *J. Alzheimers Dis. JAD* **29**, 171–176.

86 Flagmeier P, De S, Wirthensohn DC, Lee SF, Vincke C, Muyldermans S, Knowles TPJ, Gandhi S, Dobson CM & Klenerman D (2017) Ultrasensitive Measurement of Ca2+ Influx into Lipid Vesicles Induced by Protein Aggregates. *Angew. Chem. Int. Ed.*, n/a–n/a.

87 Pauwels K, Williams TL, Morris KL, Jonckheere W, Vandersteen A, Kelly G, Schymkowitz J, Rousseau F, Pastore A, Serpell LC & Broersen K (2012) Structural basis for increased toxicity of pathological Aβ42:Aβ40 ratios in alzheimer disease. *J. Biol. Chem.* **287**, 5650–5660.

88 Shankar GM, Walsh DM, Walsh D, Rowan M, Schoemaker H, Draguhn A, Wicke K, Nimmrich V, Bitner R, Harlan J, Barlow E, Ebert U, Hillen H, Walter K, Johnson R, Hajduk P & Olejniczak E (2009) Alzheimer's disease: synaptic dysfunction and Aβ. *Mol. Neurodegener.* **4**, 48.

89 Walsh DM, Lomakin A, Benedek GB, Condron MM & Teplow DB (1997) Amyloid ??-protein fibrillogenesis: Detection of a protofibrillar intermediate. *J. Biol. Chem.* **272**, 22364–22372.

90 Walsh DM, Hartley DM, Kusumoto Y, Fezoui Y, Condron MM, Lomakin A, Benedek GB, Selkoe DJ & Teplow DB (1999) Amyloid beta-protein fibrillogenesis. Structure and biological activity of protofibrillar intermediates. *J. Biol. Chem.* **274**, 25945–52.

91 Hepler RW, Grimm KM, Nahas DD, Breese R, Dodson EC, Acton P, Keller PM, Yeager M, Wang H, Shughrue P, Kinney G & Joyce JG (2006) Solution State Characterization of Amyloid β-Derived Diffusible Ligands. *Biochemistry (Mosc.)* **45**, 15157–15167.

92 Laurén J, Gimbel DA, Nygaard HB, Gilbert JW & Strittmatter SM (2009) Cellular prion protein mediates impairment of synaptic plasticity by amyloid-β oligomers. *Nature* **457**, 1128–1132.

93 Yu L, Edalji R, Harlan JE, Holzman TF, Lopez AP, Labkovsky B, Hillen H, Barghorn S, Ebert U, Richardson PL, Miesbauer L, Solomon L, Bartley D, Walter K, Johnson RW, Hajduk PJ & Olejniczak ET (2009) Structural Characterization of a Soluble Amyloid β-Peptide Oligomer. *Biochemistry (Mosc.)* **48**, 1870–1877.

94 Hoshi M, Sato M, Matsumoto S, Noguchi A, Yasutake K, Yoshida N & Sato K (2003) Spherical aggregates of  -amyloid (amylospheroid) show high neurotoxicity and activate tau protein kinase I/glycogen synthase kinase-3. *Proc. Natl. Acad. Sci.* **100**, 6370–6375.

95 Noguchi A, Matsumura S, Dezawa M, Tada M, Yanazawa M, Ito A, Akioka M, Kikuchi S, Sato M, Ideno S, Noda M, Fukunari A, Muramatsu S, Itokazu Y, Sato K, Takahashi H, Teplow DB, Nabeshima Y, Kakita A, Imahori K & Hoshi M (2009) Isolation and Characterization of Patient-derived, Toxic, High Mass Amyloid β-Protein (Aβ) Assembly from Alzheimer Disease Brains. *J. Biol. Chem.* **284**, 32895–32905.

96 Walsh DM, Townsend M, Podlisny MB, Shankar GM, Fadeeva J V, El Agnaf O, Hartley DM & Selkoe DJ (2005) Certain inhibitors of synthetic amyloid beta-peptide (Abeta) fibrillogenesis block oligomerization of natural Abeta and thereby rescue long-term potentiation. *J. Neurosci. Off. J. Soc. Neurosci.* **25**, 2455–2462.

97 Podlisny MB, Ostaszewski BL, Squazzo SL, Koo EH, Rydell RE, Teplow DB & Selkoe DJ (1995) Aggregation of secreted amyloid beta-protein into sodium dodecyl sulfate-stable oligomers in cell culture. *J. Biol. Chem.* **270**, 9564–9570.

98 Lesné S, Koh MT, Kotilinek L, Kayed R, Glabe CG, Yang A, Gallagher M & Ashe KH (2006) A specific amyloid-β protein assembly in the brain impairs memory. *Nature* **440**, 352–357.

99 Stroud JC, Liu C, Teng PK & Eisenberg D (2012) Toxic fibrillar oligomers of amyloid-β have cross-β structure. *Proc. Natl. Acad. Sci. U. S. A.* **109**, 7717–7722.

100 Ahmed M, Davis J, Aucoin D, Sato T, Ahuja S, Aimoto S, Elliott JI, Van Nostrand WE & Smith SO (2010) Structural conversion of neurotoxic amyloid-beta(1-42) oligomers to fibrils. *Nat. Struct. Mol. Biol.* **17**, 561–567.

101 Harper JD, Lieber CM & Lansbury PT (1997) Atomic force microscopic imaging of seeded fibril formation and fibril branching by the Alzheimer's disease amyloid-beta protein. *Chem. Biol.* **4**, 951–959.

102 Parbhu A, Lin H, Thimm J & Lal R (2002) Imaging real-time aggregation of amyloid beta protein (1-42) by atomic force microscopy. *Peptides* **23**, 1265–1270.

103 Bartolini M, Naldi M, Fiori J, Valle F, Biscarini F, Nicolau DV & Andrisano V (2011) Kinetic characterization of amyloid-beta 1-42 aggregation with a multimethodological approach. *Anal. Biochem.* **414**, 215–225.

104 Yates EA, Cucco EM & Legleiter J (2011) Point mutations in Aβ induce polymorphic aggregates at liquid/solid interfaces. *ACS Chem. Neurosci.* **2**, 294–307.

105 Ruggeri FS, Adamcik J, Jeong JS, Lashuel HA, Mezzenga R & Dietler G (2015) Influence of the β-Sheet Content on the Mechanical Properties of Aggregates during Amyloid Fibrillization. *Angew. Chem. Int. Ed.* **54**, 2462–2466.

106 Lu J-X, Qiang W, Yau W-M, Schwieters CD, Meredith SC & Tycko R (2013) Molecular Structure of β-Amyloid Fibrils in Alzheimer's Disease Brain Tissue. *Cell* **154**, 1257–1268.

107 Colvin MT, Silvers R, Ni QZ, Can TV, Sergeyev I, Rosay M, Donovan KJ, Michael B, Wall J, Linse S & Griffin RG (2016) Atomic Resolution Structure of Monomorphic Aβ42 Amyloid Fibrils. *J. Am. Chem. Soc.* **138**, 9663–9674.

108 Qiang W, Yau W-M, Lu J-X, Collinge J & Tycko R (2017) Structural variation in amyloid-β fibrils from Alzheimer's disease clinical subtypes. *Nature* **541**, 217–221.

109 Eisenberg D & Jucker M (2012) The Amyloid State of Proteins in Human Diseases. *Cell* **148**, 1188–1203.

110 Gremer L, Schölzel D, Schenk C, Reinartz E, Labahn J, Ravelli RBG, Tusche M, Lopez-Iglesias C, Hoyer W, Heise H, Willbold D & Schröder GF (2017) Fibril structure of amyloid-β(1–42) by cryo–electron microscopy. *Science* **358**, 116–119.

111 Ding H, Wong PT, Lee EL, Gafni A & Steel DG (2009) Determination of the oligomer size of amyloidogenic protein beta-amyloid(1-40) by single-molecule spectroscopy. *Biophys. J.* **97**, 912–21.

112 Narayan P, Meehan S, Carver JA, Wilson MR, Dobson CM & Klenerman D (2012) Amyloid-β Oligomers are Sequestered by both Intracellular and Extracellular Chaperones. *Biochemistry (Mosc.)* **51**, 9270–9276.

113 Narayan P, Orte A, Clarke RW, Bolognesi B, Hook S, Ganzinger KA, Meehan S, Wilson MR, Dobson CM & Klenerman D (2012) The extracellular chaperone clusterin sequesters oligomeric forms of the amyloid-β(1-40) peptide. *Nat. Struct. Mol. Biol.* **19**, 79–83.

114 Narayan P, Holmström KM, Kim D-H, Whitcomb DJ, Wilson MR, St. George-Hyslop P, Wood NW, Dobson CM, Cho K, Abramov AY & Klenerman D (2014) Rare Individual Amyloid-β Oligomers Act on Astrocytes to Initiate Neuronal Damage. *Biochemistry (Mosc.)* **53**, 2442–2453.

115 Narayan P, Meehan S, Carver JA, Wilson MR, Dobson CM & Klenerman D (2012) Amyloid-β Oligomers are Sequestered by both Intracellular and Extracellular Chaperones. *Biochemistry (Mosc.)* **51**, 9270–9276.

116 Narayan P, Ganzinger KA, McColl J, Weimann L, Meehan S, Qamar S, Carver JA, Wilson MR, St. George-Hyslop P, Dobson CM & Klenerman D (2013) Single Molecule Characterization of the Interactions between Amyloid-β Peptides and the Membranes of Hippocampal Cells. *J. Am. Chem. Soc.* **135**, 1491–1498.

117 Ding H, Wong PT, Lee EL, Gafni A & Steel DG (2009) Determination of the oligomer size of amyloidogenic protein beta-amyloid(1-40) by single-molecule spectroscopy. *Biophys. J.* **97**, 912–21.

118 Iljina M, Garcia GA, Dear AJ, Flint J, Narayan P, Michaels TCT, Dobson CM, Frenkel D, Knowles TPJ & Klenerman D (2016) Quantitative analysis of co-oligomer formation by amyloid-beta peptide isoforms. *Sci. Rep.* **6**, 28658.

119 Murphy RR, Danezis G, Horrocks MH, Jackson SE & Klenerman D (2014) Bayesian Inference of Accurate Population Sizes and FRET Efficiencies from Single Diffusing Biomolecules. *Anal. Chem.* **86**, 8603–8612.

120 Kaminski Schierle GS, van de Linde S, Erdelyi M, Esbjörner EK, Klein T, Rees E, Bertoncini CW, Dobson CM, Sauer M & Kaminski CF (2011) In Situ Measurements of the Formation and Morphology of Intracellular β-Amyloid Fibrils by Super-Resolution Fluorescence Imaging. *J. Am. Chem. Soc.* **133**, 12902–12905.

121 Zhang WI, Antonios G, Rabano A, Bayer TA, Schneider A & Rizzoli SO (2015) Super-Resolution Microscopy of Cerebrospinal Fluid Biomarkers as a Tool for Alzheimer's Disease Diagnostics. *J. Alzheimers Dis. JAD*.

122 Fritschi S, Langer F, Kaeser S, Maia L, Portelius E, Pinotsi D, Winkler D, Maetzler W, Keyvani K, Spitzer P, Wiltfang J, Kaminski-Schierle G, Zetterberg H, Staufenbiehl M & Jucker M (2014) Highly potent soluble Abeta seeds in human Alzheimer brain but not cerebrospinal fluid. *Brain*.

123 Brelstaff J, Ossola B, Neher JJ, Klingstedt T, Nilsson KPR, Goedert M, Spillantini MG & Tolkovsky AM (2015) The fluorescent pentameric oligothiophene pFTAA identifies filamentous tau in live neurons cultured from adult P301S tau mice. *Front. Neurosci.* **9**, 1–12.

124 Aslund A, Sigurdson CJ, Klingstedt T, Grathwohl S, Bolmont T, Dickstein DL, Glimsdal E, Prokop S, Lindgren M, Konradsson P, Holtzman DM, Hof PR, Heppner FL, Gandy S, Jucker M, Aguzzi A, Hammarström P & Nilsson KPR (2009) Novel pentameric thiophene derivatives for in vitro and in vivo optical imaging of a plethora of protein aggregates in cerebral amyloidoses. *ACS Chem. Biol.* **4**, 673–84.

125 Klingstedt T, Aslund A, Simon RA, Johansson LBG, Mason JJ, Nyström S, Hammarström P & Nilsson KPR (2011) Synthesis of a library of oligothiophenes and their utilization as

fluorescent ligands for spectral assignment of protein aggregates. *Org. Biomol. Chem.* **9**, 8356–70.

126 Klingstedt T, Shirani H, Andreas KO, Cairns NJ, Sigurdson CJ, Goedert M & Nilsson KPR (2013) The Structural Basis for Optimal Performance of Oligothiophene-Based Fluorescent Amyloid Ligands : Conformational Flexibility is Essential for Spectral Assignment of a Diversity of Protein Aggregates. , 10179–10192.

127 Hellstrand E, Boland B, Walsh DM & Linse S (2010) Amyloid β-protein aggregation produces highly reproducible kinetic data and occurs by a two-phase process. *ACS Chem. Neurosci.* **1**, 13–8.

128 Meisl G, Kirkegaard JB, Arosio P, Michaels TCT, Vendruscolo M, Dobson CM, Linse S & Knowles TPJ (2016) Molecular mechanisms of protein aggregation from global fitting of kinetic models. *Nat. Protoc.* **11**, 252–272.

129 Meisl G, Yang X, Frohm B, Knowles TPJ, Linse S, Glenner GG, Wong CW, Hardy J, Allsop D, Knowles TP, Vendruscolo M, Dobson CM, Walsh DM, Jan A, Cohen SI, Meisl G, Arosio P, Cukalevski C, Frohm B, Knowles TPJ, Linse S, Cohen SIA, Fede G Di, Diomede L, Messa M, Buell AK, Walsh DM, Cabaleiro-Lago C, Cabaleiro-Lago C, Lynch I, Quinlan-Pluck F, Dawson K, Linse S, Vácha R, Linse S, Lund M, Shen L, Morinaga A, Hellstrand E, Boland B, Walsh D, Linse S, Cukalevski R, Knowles TPJ, Cohen SI, Vendruscolo M, Dobson CM, Knowles TP, Giaccone G, Chothia C, Janin J, Wolfenden R, Andersson L, Cullis PM, Southgate CC, Oosawa F, Asakura S, Cohen SIA, Vendruscolo M, Dobson CM & Knowles TPJ (2016) Quantitative analysis of intrinsic and extrinsic factors in the aggregation mechanism of Alzheimer-associated Aβ-peptide. *Sci. Rep.* **6**, 18728.

130 Arosio P, Michaels TCT, Linse S, Månsson C, Emanuelsson C, Presto J, Johansson J, Vendruscolo M, Dobson CM & Knowles TPJ (2016) Kinetic analysis reveals the diversity of microscopic mechanisms through which molecular chaperones suppress amyloid formation. *Nat. Commun.* **7**, 10948.

131 Munke A, Persson J, Weiffert T, De Genst E, Meisl G, Arosio P, Carnerup A, Dobson CM, Vendruscolo M, Knowles TPJ & Linse S (2017) Phage display and kinetic selection of antibodies that specifically inhibit amyloid self-replication. *Proc. Natl. Acad. Sci. U. S. A.* **114**, 6444–6449.

132 Savage MJ, Kalinina J, Wolfe A, Tugusheva K, Korn R, Cash-Mason T, Maxwell JW, Hatcher NG, Haugabook SJ, Wu G, Howell BJ, Renger JJ, Shughrue PJ & McCampbell A (2014) A Sensitive Aβ Oligomer Assay Discriminates Alzheimer's and Aged Control Cerebrospinal Fluid. *J. Neurosci.* **34**, 2884–2897.

133 Goedert M (2015) Alzheimer's and Parkinson's diseases: The prion concept in relation to assembled Aβ, tau, and α-synuclein. *Science* **349**, 1255555.

134 Lee G, Cowan N & Kirschner M (1988) The primary structure and heterogeneity of tau protein from mouse brain. *Science* **239**, 285–288.

135 Goedert M, Spillantini MG, Potier MC, Ulrich J & Crowther RA (1989) Cloning and sequencing of the cDNA encoding an isoform of microtubule-associated protein tau containing four tandem repeats: differential expression of tau protein mRNAs in human brain. *EMBO J.* **8**, 393–399.

136 Goedert M, Spillantini MG, Jakes R, Rutherford D & Crowther RA (1989) Multiple isoforms of human microtubule-associated protein tau: sequences and localization in neurofibrillary tangles of Alzheimer's disease. *Neuron* **3**, 519–526.

137 Himmler A (1989) Structure of the bovine tau gene: alternatively spliced transcripts generate a protein family. *Mol. Cell. Biol.* **9**, 1389–1396.

138 Himmler A, Drechsel D, Kirschner MW & Martin DW (1989) Tau consists of a set of proteins with repeated C-terminal microtubule-binding domains and variable N-terminal domains. *Mol. Cell. Biol.* **9**, 1381–1388.

139 Wang Y & Mandelkow E (2016) Tau in physiology and pathology. *Nat. Rev. Neurosci.* **17**, 22–35.

140 Poorkaj P, Bird TD, Wijsman E, Nemens E, Garruto RM, Anderson L, Andreadis A, Wiederholt WC, Raskind M & Schellenberg GD (1998) Tau is a candidate gene for chromosome 17 frontotemporal dementia. *Ann. Neurol.* **43**, 815–825.

141 Hutton M, Lendon CL, Rizzu P, Baker M, Froelich S, Houlden H, Pickering-Brown S, Chakraverty S, Isaacs A, Grover A, Hackett J, Adamson J, Lincoln S, Dickson D, Davies P, Petersen RC, Stevens M, de Graaff E, Wauters E, van Baren J, Hillebrand M, Joosse M, Kwon JM, Nowotny P, Che LK, Norton J, Morris JC, Reed LA, Trojanowski J, Basun H, Lannfelt L, Neystat M, Fahn S, Dark F, Tannenberg T, Dodd PR, Hayward N, Kwok JBJ, Schofield PR, Andreadis A,

Snowden J, Craufurd D, Neary D, Owen F, Oostra BA, Hardy J, Goate A, van Swieten J, Mann D, Lynch T & Heutink P (1998) Association of missense and 5'-splice-site mutations in tau with the inherited dementia FTDP-17. *Nature* **393**, 702–705.

142 Spillantini MG, Murrell JR, Goedert M, Farlow MR, Klug A & Ghetti B (1998) Mutation in the tau gene in familial multiple system tauopathy with presenile dementia. *Proc. Natl. Acad. Sci. U. S. A.* **95**, 7737–7741.

143 Ghetti B, Oblak AL, Boeve BF, Johnson KA, Dickerson BC & Goedert M (2015) Invited review: Frontotemporal dementia caused by microtubule-associated protein tau gene (MAPT) mutations: a chameleon for neuropathology and neuroimaging. *Neuropathol. Appl. Neurobiol.* **41**, 24–46.

144 Iqbal K, Liu F & Gong C-X (2016) Tau and neurodegenerative disease: the story so far. *Nat. Rev. Neurol.* **12**, 15–27.

145 Wischik CM, Novak M, Thøgersen HC, Edwards PC, Runswick MJ, Jakes R, Walker JE, Milstein C, Roth M & Klug A (1988) Isolation of a fragment of tau derived from the core of the paired helical filament of Alzheimer disease. *Proc. Natl. Acad. Sci. U. S. A.* **85**, 4506–4510.

146 Fitzpatrick AWP, Falcon B, He S, Murzin AG, Murshudov G, Garringer HJ, Crowther RA, Ghetti B, Goedert M & Scheres SHW (2017) Cryo-EM structures of tau filaments from Alzheimer's disease. *Nature* **547**, 185–190.

147 Ksiezak-Reding H, Liu W-K & Yen S-H (1992) Phosphate analysis and dephosphorylation of modified tau associated with paired helical filaments. *Brain Res.* **597**, 209–219.

148 Köpke E, Tung YC, Shaikh S, Alonso AC, Iqbal K & Grundke-Iqbal I (1993) Microtubule-associated protein tau. Abnormal phosphorylation of a non-paired helical filament pool in Alzheimer disease. *J. Biol. Chem.* **268**, 24374–24384.

149 Barrantes A, Sotres J, Hernando-Pérez M, Benítez MJ, de Pablo PJ, Baró AM, Avila J & Jiménez JS (2009) Tau aggregation followed by atomic force microscopy and surface plasmon resonance, and single molecule tau-tau interaction probed by atomic force spectroscopy. *J. Alzheimers Dis. JAD* **18**, 141–151.

150 Maeda S, Sahara N, Saito Y, Murayama M, Yoshiike Y, Kim H, Miyasaka T, Murayama S, Ikai A & Takashima A (2007) Granular Tau Oligomers as Intermediates of Tau Filaments†. *Biochemistry (Mosc.)* **46**, 3856–3861.

151 Xu S, Brunden KR, Trojanowski JQ & Lee VM-Y (2010) Characterization of tau fibrillization in vitro. *Alzheimers Dement. J. Alzheimers Assoc.* **6**, 110–117.

152 Maeda S, Sahara N, Saito Y, Murayama S, Ikai A & Takashima A (2006) Increased levels of granular tau oligomers: An early sign of brain aging and Alzheimer's disease. *Neurosci. Res.* **54**, 197–201.

153 Wegmann S, Jung YJ, Chinnathambi S, Mandelkow E-M, Mandelkow E & Muller DJ (2010) Human Tau Isoforms Assemble into Ribbon-like Fibrils That Display Polymorphic Structure and Stability. *J. Biol. Chem.* **285**, 27302–27313.

154 Wegmann S, Medalsy ID, Mandelkow E & Müller DJ (2013) The fuzzy coat of pathological human Tau fibrils is a two-layered polyelectrolyte brush. *Proc. Natl. Acad. Sci. U. S. A.* **110**, E313–E321.

155 Medalsy I, Hensen U & Muller DJ (2011) Imaging and Quantifying Chemical and Physical Properties of Native Proteins at Molecular Resolution by Force–Volume AFM. *Angew. Chem. Int. Ed.* **50**, 12103–12108.

156 von Bergen M, Barghorn S, Müller SA, Pickhardt M, Biernat J, Mandelkow E-M, Davies P, Aebi U & Mandelkow E (2006) The Core of Tau-Paired Helical Filaments Studied by Scanning Transmission Electron Microscopy and Limited Proteolysis. *Biochemistry (Mosc.)* **45**, 6446–6457.

157 Crowther RA (1991) Straight and paired helical filaments in Alzheimer disease have a common structural unit. *Proc. Natl. Acad. Sci. U. S. A.* **88**, 2288–2292.

158 Friedhoff P, Bergen M von, Mandelkow E-M, Davies P & Mandelkow E (1998) A nucleated assembly mechanism of Alzheimer paired helical filaments. *Proc. Natl. Acad. Sci. U. S. A.* **95**, 15712–15717.

159 Congdon EE, Kim S, Bonchak J, Songrug T, Matzavinos A & Kuret J (2008) Nucleation-dependent Tau Filament Formation THE IMPORTANCE OF DIMERIZATION AND AN ESTIMATION OF ELEMENTARY RATE CONSTANTS. *J. Biol. Chem.* **283**, 13806–13816.

160 Carlson SW, Branden M, Voss K, Sun Q, Rankin CA & Gamblin TC (2007) A complex mechanism for inducer mediated tau polymerization. *Biochemistry (Mosc.)* **46**, 8838–8849.

161 King ME, Ahuja V, Binder LI & Kuret J (1999) Ligand-dependent tau filament formation: implications for Alzheimer's disease progression. *Biochemistry (Mosc.)* **38**, 14851–14859.

162 Barghorn S & Mandelkow E (2002) Toward a unified scheme for the aggregation of tau into Alzheimer paired helical filaments. *Biochemistry (Mosc.)* **41**, 14885–14896.

163 Ramachandran G & Udgaonkar JB (2011) Understanding the kinetic roles of the inducer heparin and of rod-like protofibrils during amyloid fibril formation by Tau protein. *J. Biol. Chem.* **286**, 38948–38959.

164 Elbaum-Garfinkle S & Rhoades E (2012) Identification of an aggregation-prone structure of tau. *J. Am. Chem. Soc.* **134**, 16607–16613.

165 Shammas SL, Garcia GA, Kumar S, Kjaergaard M, Horrocks MH, Shivji N, Mandelkow E, Knowles TPJ, Mandelkow E & Klenerman D (2015) A mechanistic model of tau amyloid aggregation based on direct observation of oligomers. *Nat. Commun.* **6**, 7025.

166 Kumar S, Tepper K, Kaniyappan S, Biernat J, Wegmann S, Mandelkow E-M, Muller DJ & Mandelkow E (2014) Stages and Conformations of the Tau Repeat Domain during Aggregation and Its Effect on Neuronal Toxicity. *J. Biol. Chem.* **289**, 20318–20332.

167 Cremades N, Cohen SIA, Deas E, Abramov AY, Chen AY, Orte A, Sandal M, Clarke RW, Dunne P, Aprile FA, Bertoncini CW, Wood NW, Knowles TPJ, Dobson CM & Klenerman D (2012) Direct Observation of the Interconversion of Normal and Toxic Forms of α-Synuclein. *Cell* **149**, 1048–1059.

168 Lewis J, McGowan E, Rockwood J, Melrose H, Nacharaju P, Van Slegtenhorst M, Gwinn-Hardy K, Paul Murphy M, Baker M, Yu X, Duff K, Hardy J, Corral A, Lin WL, Yen SH, Dickson DW, Davies P & Hutton M (2000) Neurofibrillary tangles, amyotrophy and progressive motor disturbance in mice expressing mutant (P301L) tau protein. *Nat. Genet.* **25**, 402–405.

169 Ramachandran G & Udgaonkar JB (2012) Evidence for the existence of a secondary pathway for fibril growth during the aggregation of tau. *J. Mol. Biol.* **421**, 296–314.

170 Kundel F, De S, Flagmeier P, Horrocks MH, Kjaergaard M, Shammas SL, Jackson SE, Dobson CM & Klenerman D (2018) Hsp70 Inhibits the Nucleation and Elongation of Tau and Sequesters Tau Aggregates with High Affinity. *ACS Chem. Biol.*

171 Baughman HER, Clouser AF, Klevit RE & Nath A (2018) HspB1 and Hsc70 chaperones engage distinct tau species and have different inhibitory effects on amyloid formation. *J. Biol. Chem.*, jbc.M117.803411.

172 Bader B, Nübling G, Mehle A, Nobile S, Kretzschmar H & Giese A (2011) Single particle analysis of tau oligomer formation induced by metal ions and organic solvents. *Biochem. Biophys. Res. Commun.* **411**, 190–196.

173 Nubling G, Bader B, Levin J, Hildebrandt J, Kretzschmar H & Giese A (2012) Synergistic influence of phosphorylation and metal ions on tau oligomer formation and coaggregation with ?-synuclein at the single molecule level. *Mol. Neurodegener.* **7**, 35.

174 Nübling G, Levin J, Bader B, Israel L, Bötzel K, Lorenzl S & Giese A (2012) Limited cleavage of tau with matrix-metalloproteinase MMP-9, but not MMP-3, enhances tau oligomer formation. *Exp. Neurol.* **237**, 470–476.

175 Elbaum-Garfinkle S, Ramlall T & Rhoades E (2010) The role of the lipid bilayer in tau aggregation. *Biophys. J.* **98**, 2722–2730.

176 Jeganathan S, von Bergen M, Brutlach H, Steinhoff H-J & Mandelkow E (2006) Global hairpin folding of tau in solution. *Biochemistry (Mosc.)* **45**, 2283–2293.

177 Nath S, Meuvis J, Hendrix J, Carl SA & Engelborghs Y (2010) Early Aggregation Steps in α-Synuclein as Measured by FCS and FRET: Evidence for a Contagious Conformational Change. *Biophys. J.* **98**, 1302–1311.

178 Kaminski Schierle GS, Bertoncini CW, Chan FTS, van der Goot AT, Schwedler S, Skepper J, Schlachter S, van Ham T, Esposito A, Kumita JR, Nollen EAA, Dobson CM & Kaminski CF (2011) A FRET sensor for non-invasive imaging of amyloid formation in vivo. *Eur. J. Chem. Phys. Phys. Chem.* **12**, 673–680.

179 Michel CH, Kumar S, Pinotsi D, Tunnacliffe A, St. George-Hyslop P, Mandelkow E, Mandelkow E-M, Kaminski CF & Kaminski Schierle GS (2014) Extracellular Monomeric Tau Protein Is Sufficient to Initiate the Spread of Tau Protein Pathology. *J. Biol. Chem.* **289**, 956–967.

180 Chen W, Young LJ, Lu M, Zaccone A, Ströhl F, Yu N, Kaminski Schierle GS & Kaminski CF (2017) Fluorescence Self-Quenching from Reporter Dyes Informs on the Structural Properties of Amyloid Clusters Formed in Vitro and in Cells. *Nano Lett.* **17**, 143–149.

181 Benda A, Aitken H, Davies DS, Whan R & Goldsbury C (2016) STED imaging of tau filaments in Alzheimer's disease cortical grey matter. *J. Struct. Biol.* **195**, 345–352.

182 Jakes R, Spillantini MG & Goedert M (1994) Identification of two distinct synucleins from human brain. *FEBS Lett.* **345**, 27–32.

183 Chartier-Harlin M-C, Kachergus J, Roumier C, Mouroux V, Douay X, Lincoln S, Levecque C, Larvor L, Andrieux J, Hulihan M, Waucquier N, Defebvre L, Amouyel P, Farrer M & Destée A (2004) Alpha-synuclein locus duplication as a cause of familial Parkinson's disease. *Lancet* **364**, 1167–1169.

184 Singleton AB, Farrer M, Johnson J, Singleton A, Hague S, Kachergus J, Hulihan M, Peuralinna T, Dutra A, Nussbaum R, Lincoln S, Crawley A, Hanson M, Maraganore D, Adler C, Cookson MR, Muenter M, Baptista M, Miller D, Blancato J, Hardy J & Gwinn-Hardy K (2003) α-Synuclein Locus Triplication Causes Parkinson's Disease. *Science* **302**, 841.

185 Polymeropoulos MH, Lavedan C, Leroy E, Ide SE, Dehejia A, Dutra A, Pike B, Root H, Rubenstein J, Boyer R, Stenroos ES, Chandrasekharappa S, Athanassiadou A, Papapetropoulos T, Johnson WG, Lazzarini AM, Duvoisin RC, Di Iorio G, Golbe LI & Nussbaum RL (1997) Mutation in the alpha-synuclein gene identified in families with Parkinson's disease. *Science* **276**, 2045–2047.

186 Krüger R, Kuhn W, Müller T, Woitalla D, Graeber M, Kösel S, Przuntek H, Epplen JT, Schöls L & Riess O (1998) Ala30Pro mutation in the gene encoding alpha-synuclein in Parkinson's disease. *Nat. Genet.* **18**, 106–108.

187 Zarranz JJ, Alegre J, Gómez-Esteban JC, Lezcano E, Ros R, Ampuero I, Vidal L, Hoenicka J, Rodriguez O, Atarés B, Llorens V, Gomez Tortosa E, del Ser T, Muñoz DG & de Yebenes JG (2004) The new mutation, E46K, of alpha-synuclein causes Parkinson and Lewy body dementia. *Ann. Neurol.* **55**, 164–173.

188 Proukakis C, Dudzik CG, Brier T, MacKay DS, Cooper JM, Millhauser GL, Houlden H & Schapira AH (2013) A novel α-synuclein missense mutation in Parkinson disease. *Neurology* **80**, 1062–1064.

189 Kiely AP, Asi YT, Kara E, Limousin P, Ling H, Lewis P, Proukakis C, Quinn N, Lees AJ, Hardy J, Revesz T, Houlden H & Holton JL (2013) α-Synucleinopathy associated with G51D SNCA mutation: a link between Parkinson's disease and multiple system atrophy? *Acta Neuropathol. (Berl.)* **125**, 753–769.

190 Pasanen P, Myllykangas L, Siitonen M, Raunio A, Kaakkola S, Lyytinen J, Tienari PJ, Pöyhönen M & Paetau A (2014) A novel α-synuclein mutation A53E associated with atypical multiple system atrophy and Parkinson's disease-type pathology. *Neurobiol. Aging* **35**, 2180.e1–5.

191 Eliezer D, Kutluay E, Bussell R Jr & Browne G (2001) Conformational properties of alpha-synuclein in its free and lipid-associated states. *J. Mol. Biol.* **307**, 1061–1073.

192 Bussell R Jr & Eliezer D (2003) A structural and functional role for 11-mer repeats in alpha-synuclein and other exchangeable lipid binding proteins. *J. Mol. Biol.* **329**, 763–778.

193 Han H, Weinreb PH & Lansbury PT (1995) The core Alzheimer's peptide NAC forms amyloid fibrils which seed and are seeded by beta-amyloid: is NAC a common trigger or target in neurodegenerative disease? *Chem. Biol.* **2**, 163–169.

194 Giasson BI, Murray IV, Trojanowski JQ & Lee VM (2001) A hydrophobic stretch of 12 amino acid residues in the middle of alpha-synuclein is essential for filament assembly. *J. Biol. Chem.* **276**, 2380–2386.

195 Hoyer W, Cherny D, Subramaniam V & Jovin TM (2004) Impact of the acidic C-terminal region comprising amino acids 109-140 on alpha-synuclein aggregation in vitro. *Biochemistry (Mosc.)* **43**, 16233–16242.

196 Uversky VN (2003) A protein-chameleon: conformational plasticity of alpha-synuclein, a disordered protein involved in neurodegenerative disorders. *J. Biomol. Struct. Dyn.* **21**, 211–234.

197 Lee A & Gilbert RM (2016) Epidemiology of Parkinson Disease. *Neurol. Clin.* **34**, 955–965.

198 Bussell R Jr & Eliezer D (2001) Residual structure and dynamics in Parkinson's disease-associated mutants of alpha-synuclein. *J. Biol. Chem.* **276**, 45996–46003.

199 Greenbaum EA, Graves CL, Mishizen-Eberz AJ, Lupoli MA, Lynch DR, Englander SW, Axelsen PH & Giasson BI (2005) The E46K mutation in alpha-synuclein increases amyloid fibril formation. *J. Biol. Chem.* **280**, 7800–7807.

200 Li J, Uversky VN & Fink AL (2001) Effect of familial Parkinson's disease point mutations A30P and A53T on the structural properties, aggregation, and fibrillation of human alpha-synuclein. *Biochemistry (Mosc.)* **40**, 11604–11613.

201 Fares M-B, Ait-Bouziad N, Dikiy I, Mbefo MK, Jovičić A, Kiely A, Holton JL, Lee S-J, Gitler AD, Eliezer D & Lashuel HA (2014) The novel Parkinson's disease linked mutation G51D attenuates in vitro aggregation and membrane binding of α-synuclein, and enhances its secretion and nuclear localization in cells. *Hum. Mol. Genet.* **23**, 4491–4509.

202 Ghosh D, Mondal M, Mohite GM, Singh PK, Ranjan P, Anoop A, Ghosh S, Jha NN, Kumar A & Maji SK (2013) The Parkinson's disease-associated H50Q mutation accelerates α-Synuclein aggregation in vitro. *Biochemistry (Mosc.)* **52**, 6925–6927.

203 Ghosh D, Sahay S, Ranjan P, Salot S, Mohite GM, Singh PK, Dwivedi S, Carvalho E, Banerjee R, Kumar A & Maji SK (2014) The newly discovered parkinson's disease associated finnish mutation (A53E) attenuates α-synuclein aggregation and membrane binding. *Biochemistry (Mosc.)* **53**, 6419–6421.

204 Conway KA, Harper JD & Lansbury PT (1998) Accelerated in vitro fibril formation by a mutant alpha-synuclein linked to early-onset Parkinson disease. *Nat. Med.* **4**, 1318–1320.

205 Lashuel HA, Petre BM, Wall J, Simon M, Nowak RJ, Walz T & Lansbury PT Jr (2002) Alpha-synuclein, especially the Parkinson's disease-associated mutants, forms pore-like annular and tubular protofibrils. *J. Mol. Biol.* **322**, 1089–1102.

206 Giehm L, Svergun DI, Otzen DE & Vestergaard B (2011) Low-resolution structure of a vesicle disrupting α-synuclein oligomer that accumulates during fibrillation. *Proc. Natl. Acad. Sci. U. S. A.* **108**, 3246–3251.

207 Chen SW, Drakulic S, Deas E, Ouberai M, Aprile FA, Arranz R, Ness S, Roodveldt C, Guilliams T, De-Genst EJ, Klenerman D, Wood NW, Knowles TPJ, Alfonso C, Rivas G, Abramov AY, Valpuesta JM, Dobson CM & Cremades N (2015) Structural characterization of toxic oligomers that are kinetically trapped during α-synuclein fibril formation. *Proc. Natl. Acad. Sci. U. S. A.*

208 Lorenzen N, Nielsen SB, Buell AK, Kaspersen JD, Arosio P, Vad BS, Paslawski W, Christiansen G, Valnickova-Hansen Z, Andreasen M, Enghild JJ, Pedersen JS, Dobson CM, Knowles TPJ &

Otzen DE (2014) The role of stable α-synuclein oligomers in the molecular events underlying amyloid formation. *J. Am. Chem. Soc.* **136**, 3859–3868.

209 van Rooijen BD, Claessens MMAE & Subramaniam V (2008) Membrane binding of oligomeric alpha-synuclein depends on bilayer charge and packing. *FEBS Lett.* **582**, 3788–3792.

210 Celej MS, Sarroukh R, Goormaghtigh E, Fidelio G, Ruysschaert J-M & Raussens V (2012) Toxic prefibrillar α-synuclein amyloid oligomers adopt a distinctive antiparallel β-sheet structure. *Biochem. J.*

211 Cappai R, Leck S-L, Tew DJ, Williamson NA, Smith DP, Galatis D, Sharples RA, Curtain CC, Ali FE, Cherny RA, Culvenor JG, Bottomley SP, Masters CL, Barnham KJ & Hill AF (2005) Dopamine promotes alpha-synuclein aggregation into SDS-resistant soluble oligomers via a distinct folding pathway. *FASEB J. Off. Publ. Fed. Am. Soc. Exp. Biol.* **19**, 1377–1379.

212 Fonseca-Ornelas L, Schmidt C, Camacho-Zarco AR, Fernandez CO, Becker S & Zweckstetter M (2017) Small-Molecule-Induced Soluble Oligomers of α-Synuclein with Helical Structure. *Chem. Weinh. Bergstr. Ger.* **23**, 13010–13014.

213 Ehrnhoefer DE, Bieschke J, Boeddrich A, Herbst M, Masino L, Lurz R, Engemann S, Pastore A & Wanker EE (2008) EGCG redirects amyloidogenic polypeptides into unstructured, off-pathway oligomers. *Nat. Struct. Mol. Biol.* **15**, 558–566.

214 Pieri L, Madiona K & Melki R (2016) Structural and functional properties of prefibrillar α-synuclein oligomers. *Sci. Rep.* **6**, 24526.

215 Planchard MS, Exley SE, Morgan SE & Rangachari V (2014) Dopamine-induced α-synuclein oligomers show self- and cross-propagation properties. *Protein Sci. Publ. Protein Soc.* **23**, 1369–1379.

216 Danzer KM, Haasen D, Karow AR, Moussaud S, Habeck M, Giese A, Kretzschmar H, Hengerer B & Kostka M (2007) Different Species of α-Synuclein Oligomers Induce Calcium Influx and Seeding. *J. Neurosci.* **27**, 9220–9232.

217 Leong SL, Cappai R, Barnham KJ & Pham CLL (2009) Modulation of alpha-synuclein aggregation by dopamine: a review. *Neurochem. Res.* **34**, 1838–1846.

218 Bisaglia M, Tosatto L, Munari F, Tessari I, de Laureto PP, Mammi S & Bubacco L (2010) Dopamine quinones interact with alpha-synuclein to form unstructured adducts. *Biochem. Biophys. Res. Commun.* **394**, 424–428.

219 Rekas A, Knott RB, Sokolova A, Barnham KJ, Perez KA, Masters CL, Drew SC, Cappai R, Curtain CC & Pham CLL (2010) The structure of dopamine induced alpha-synuclein oligomers. *Eur. Biophys. J. EBJ* **39**, 1407–1419.

220 De Franceschi G, Frare E, Pivato M, Relini A, Penco A, Greggio E, Bubacco L, Fontana A & de Laureto PP (2011) Structural and morphological characterization of aggregated species of α-synuclein induced by docosahexaenoic acid. *J. Biol. Chem.* **286**, 22262–22274.

221 Iljina M, Tosatto L, Choi ML, Sang JC, Ye Y, Hughes CD, Bryant CE, Gandhi S & Klenerman D (2016) Arachidonic acid mediates the formation of abundant alpha-helical multimers of alpha-synuclein. *Sci. Rep.* **6**, 33928.

222 Paslawski W, Andreasen M, Nielsen SB, Lorenzen N, Thomsen K, Kaspersen JD, Pedersen JS & Otzen DE (2014) High stability and cooperative unfolding of α-synuclein oligomers. *Biochemistry (Mosc.)* **53**, 6252–6263.

223 Schmidt F, Levin J, Kamp F, Kretzschmar H, Giese A & Bötzel K (2012) Single-channel electrophysiology reveals a distinct and uniform pore complex formed by α-synuclein oligomers in lipid membranes. *PloS One* **7**, e42545.

224 Stefanovic AND, Lindhoud S, Semerdzhiev SA, Claessens MMAE & Subramaniam V (2015) Oligomers of Parkinson's Disease-Related α-Synuclein Mutants Have Similar Structures but Distinctive Membrane Permeabilization Properties. *Biochemistry (Mosc.)* **54**, 3142–3150.

225 Plotegher N, Berti G, Ferrari E, Tessari I, Zanetti M, Lunelli L, Greggio E, Bisaglia M, Veronesi M, Girotto S, Dalla Serra M, Perego C, Casella L & Bubacco L (2017) DOPAL derived alpha-synuclein oligomers impair synaptic vesicles physiological function. *Sci. Rep.* **7**, 40699.

226 Cremades N, Chen SW & Dobson CM (2017) Chapter Three - Structural Characteristics of α-Synuclein Oligomers. In *International Review of Cell and Molecular Biology* (Sandal M, ed), pp. 79–143. Academic Press.

227 Borsarelli CD, Falomir-Lockhart LJ, Ostatná V, Fauerbach JA, Hsiao H-H, Urlaub H, Paleček E, Jares-Erijman EA & Jovin TM (2012) Biophysical properties and cellular toxicity of covalent

crosslinked oligomers of α-synuclein formed by photoinduced side-chain tyrosyl radicals. *Free Radic. Biol. Med.* **53**, 1004–1015.

228 Ariesandi W, Chang C-F, Chen T-E & Chen Y-R (2013) Temperature-dependent structural changes of Parkinson's alpha-synuclein reveal the role of pre-existing oligomers in alpha-synuclein fibrillization. *PloS One* **8**, e53487.

229 Williams DM & Pukala TL (2013) Novel insights into protein misfolding diseases revealed by ion mobility-mass spectrometry. *Mass Spectrom. Rev.* **32**, 169–187.

230 Frimpong AK, Abzalimov RR, Uversky VN & Kaltashov IA (2010) Characterization of intrinsically disordered proteins with electrospray ionization mass spectrometry: conformational heterogeneity of alpha-synuclein. *Proteins* **78**, 714–722.

231 Illes-Toth E, Ramos MR, Cappai R, Dalton C & Smith DP (2015) Distinct higher-order α-synuclein oligomers induce intracellular aggregation. *Biochem. J.* **468**, 485–493.

232 Phillips AS, Gomes AF, Kalapothakis JMD, Gillam JE, Gasparavicius J, Gozzo FC, Kunath T, MacPhee C & Barran PE (2015) Conformational dynamics of α-synuclein: insights from mass spectrometry. *The Analyst* **140**, 3070–3081.

233 Leung CWT, Guo F, Hong Y, Zhao E, Kwok RTK, Leung NLC, Chen S, Vaikath NN, El-Agnaf OM, Tang Y, Gai W-P & Tang BZ (2015) Detection of oligomers and fibrils of α-synuclein by AIEgen with strong fluorescence. *Chem. Commun. Camb. Engl.* **51**, 1866–1869.

234 Kovalska VB, Losytskyy MY, Tolmachev OI, Slominskii YL, Segers-Nolten GMJ, Subramaniam V & Yarmoluk SM (2012) Tri- and pentamethine cyanine dyes for fluorescent detection of α-synuclein oligomeric aggregates. *J. Fluoresc.* **22**, 1441–1448.

235 Gallea JI & Celej MS (2014) Structural Insights into Amyloid Oligomers of the Parkinson Disease-related Protein -Synuclein. *J. Biol. Chem.* **289**, 26733–26742.

236 van Rooijen BD, van Leijenhorst-Groener KA, Claessens MM a. E & Subramaniam V (2009) Tryptophan fluorescence reveals structural features of alpha-synuclein oligomers. *J. Mol. Biol.* **394**, 826–833.

237 Giese A, Bader B, Bieschke J, Schaffar G, Odoy S, Kahle PJ, Haass C & Kretzschmar H (2005) Single particle detection and characterization of synuclein co-aggregation. *Biochem. Biophys. Res. Commun.* **333**, 1202–1210.

238 Kostka M, Högen T, Danzer KM, Levin J, Habeck M, Wirth A, Wagner R, Glabe CG, Finger S, Heinzelmann U, Garidel P, Duan W, Ross CA, Kretzschmar H & Giese A (2008) Single particle characterization of iron-induced pore-forming alpha-synuclein oligomers. *J. Biol. Chem.* **283**, 10992–11003.

239 Levin J, Högen T, Hillmer AS, Bader B, Schmidt F, Kamp F, Kretzschmar HA, Bötzel K & Giese A (2011) Generation of ferric iron links oxidative stress to α-synuclein oligomer formation. *J. Park. Dis.* **1**, 205–216.

240 Caruana M, Högen T, Levin J, Hillmer A, Giese A & Vassallo N (2011) Inhibition and disaggregation of α-synuclein oligomers by natural polyphenolic compounds. *FEBS Lett.* **585**, 1113–1120.

241 Horrocks MH, Tosatto L, Dear AJ, Garcia GA, Iljina M, Cremades N, Dalla Serra M, Knowles TPJ, Dobson CM & Klenerman D (2015) Fast Flow Microfluidics and Single-Molecule Fluorescence for the Rapid Characterization of α-Synuclein Oligomers. *Anal. Chem.* **87**, 8818–8826.

242 Sierecki E, Giles N, Bowden Q, Polinkovsky ME, Steinbeck J, Arrioti N, Rahman D, Bhumkar A, Nicovich PR, Ross I, Parton RG, Böcking T & Gambin Y (2016) Nanomolar oligomerization and selective co-aggregation of α-synuclein pathogenic mutants revealed by single-molecule fluorescence. *Sci. Rep.* **6**, 37630.

243 Iljina M, Garcia GA, Horrocks MH, Tosatto L, Choi ML, Ganzinger KA, Abramov AY, Gandhi S, Wood NW, Cremades N, Dobson CM, Knowles TPJ & Klenerman D (2016) Kinetic model of the aggregation of alpha-synuclein provides insights into prion-like spreading. *Proc. Natl. Acad. Sci.* **113**, E1206–E1215.

244 Tokuda T, Qureshi MM, Ardah MT, Varghese S, Shehab S a. S, Kasai T, Ishigami N, Tamaoka A, Nakagawa M & El-Agnaf OMA (2010) Detection of elevated levels of α-synuclein oligomers in CSF from patients with Parkinson disease. *Neurology* **75**, 1766–1772.

245 Wang X, Yu S, Li F & Feng T (2015) Detection of α-synuclein oligomers in red blood cells as a potential biomarker of Parkinson's disease. *Neurosci. Lett.* **599**, 115–119.

246 Danzer KM, Kranich LR, Ruf WP, Cagsal-Getkin O, Winslow AR, Zhu L, Vanderburg CR & McLean PJ (2012) Exosomal cell-to-cell transmission of alpha synuclein oligomers. *Mol. Neurodegener.* **7**, 42.

247 Delenclos M, Trendafilova T, Jones DR, Moussaud S, Baine A-M, Yue M, Hirst WD & McLean PJ (2015) A Rapid, Semi-Quantitative Assay to Screen for Modulators of Alpha-Synuclein Oligomerization Ex vivo. *Front. Neurosci.* **9**, 511.

248 Dimant H, Kalia SK, Kalia LV, Zhu LN, Kibuuka L, Ebrahimi-Fakhari D, McFarland NR, Fan Z, Hyman BT & McLean PJ (2013) Direct detection of alpha synuclein oligomers in vivo. *Acta Neuropathol. Commun.* **1**, 6.

249 Eckermann K, Kügler S & Bähr M (2015) Dimerization propensities of Synucleins are not predictive for Synuclein aggregation. *Biochim. Biophys. Acta* **1852**, 1658–1664.

250 Roberts RF, Wade-Martins R & Alegre-Abarrategui J (2015) Direct visualization of alpha-synuclein oligomers reveals previously undetected pathology in Parkinson's disease brain. *Brain J. Neurol.* **138**, 1642–1657.

251 Plotegher N, Gratton E & Bubacco L (2014) Number and Brightness analysis of alpha-synuclein oligomerization and the associated mitochondrial morphology alterations in live cells. *Biochim. Biophys. Acta* **1840**, 2014–2024.

252 Levin J, Hillmer AS, Högen T, McLean PJ & Giese A (2016) Intracellular formation of α-synuclein oligomers and the effect of heat shock protein 70 characterized by confocal single particle spectroscopy. *Biochem. Biophys. Res. Commun.* **477**, 76–82.

*Box 1 Definitions of aggregate species*

**Native monomer**: the protein in its original native conformation.

**Misfolded monomer**: a protein that has lost its native conformation to acquire one that is not functional and exposes hydrophobic patches.

**Oligomer**: an assembly of misfolded protein that retains solubility, ranging in size from a dimer to fibrillar species.

**Nucleus**: an aggregate from which monomer addition is thermodynamically favoured; it may coincide with any sized aggregate.

**Protofibrils**: early fibrillar species.

**Prefibrillar species**: all aggregated species less mature than fibrils, including oligomers, protofibrils and insoluble aggregates.

**Seed**: small fibril unit from which monomers can bind for fibril elongation, bypassing oligomer formation.

**Mature Fibrils**: fibrils that have complex architecture due to flanking of several protofibrils and involvement of other parts of the protein, not buried in the initial protofibril, which can interact by virtue of their proximity.

**Aggregate**: Any non-native assembly of protein, ranging from dimer to mature fibril.

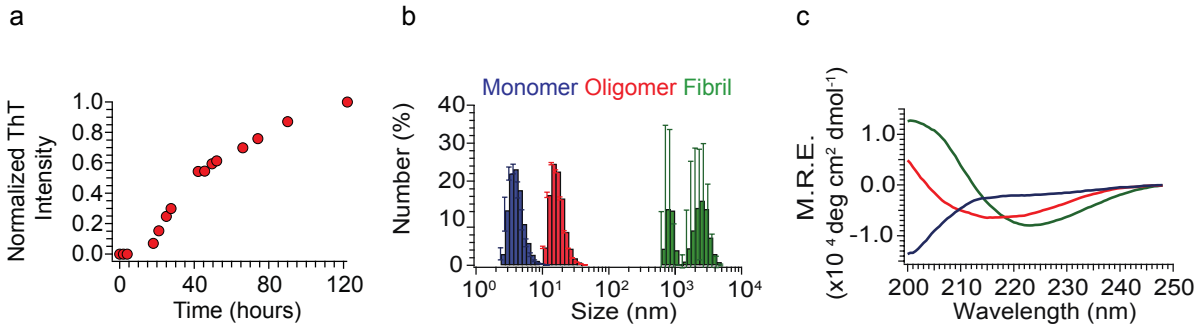


*Figure 1. Bulk techniques used to characterise the protein aggregation process. a) ThT fluorescence increase due to the aggregation of αS over time. b) Size distributions of monomeric, oligomeric and fibrillar populations of αS, measured by DLS. c) CD traces of αS monomers (blue trace), oligomers (red trace) and fibrils (green trace). (b) and (c) are adapted with permission from Horrocks et al. [51].*

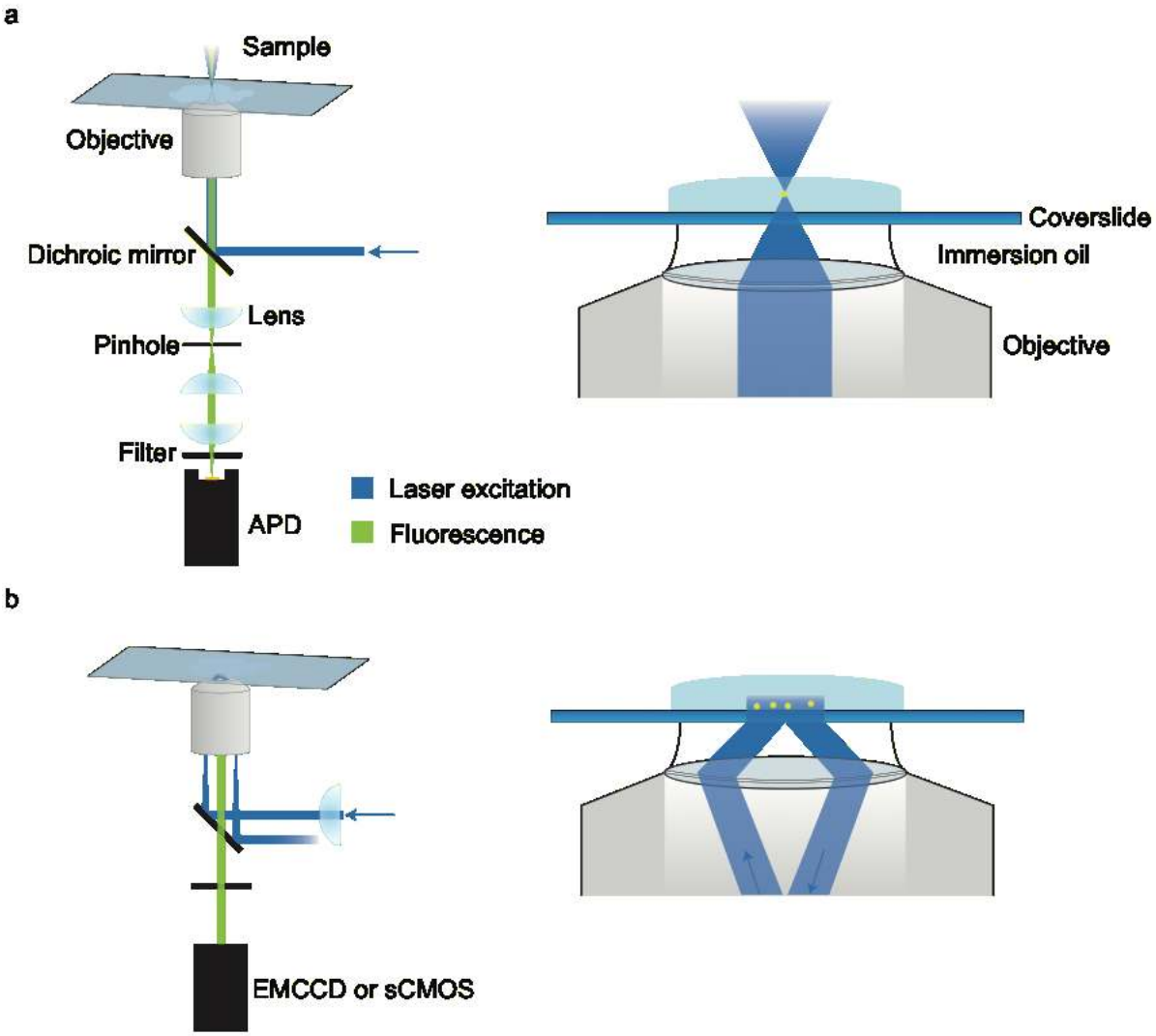


*Figure 2. Schematic of (a) a confocal microscope setup and (b) an objective-based TIRF microscope.*

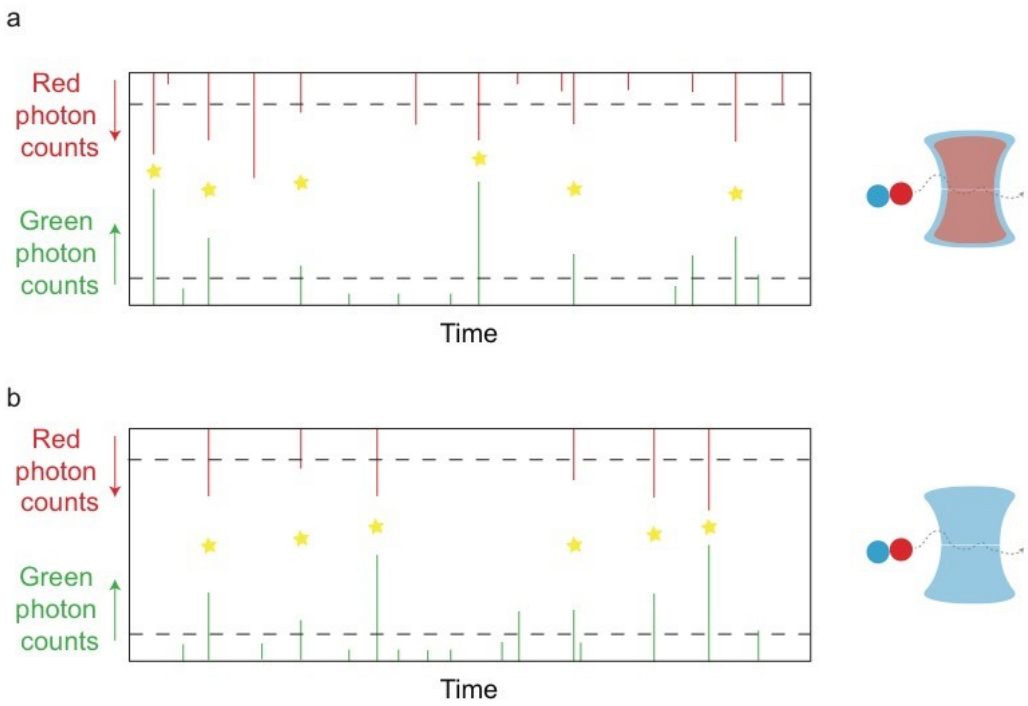


*Figure 3. TCCD and smFRET for the ultrasensitive detection of protein aggregates a) In TCCD, two colour excitation is used to excite molecules transiting the confocal volume. Only those which contain both dyes give rise to coincident bursts (yellow stars). b) In FRET based measurements, only one wavelength of light is used to excite the molecules. In molecules in which the two dyes are close enough for FRET to occur, there is a simultaneous burst in both channels. The dashed lines represent thresholds used to separate signal from noise.*

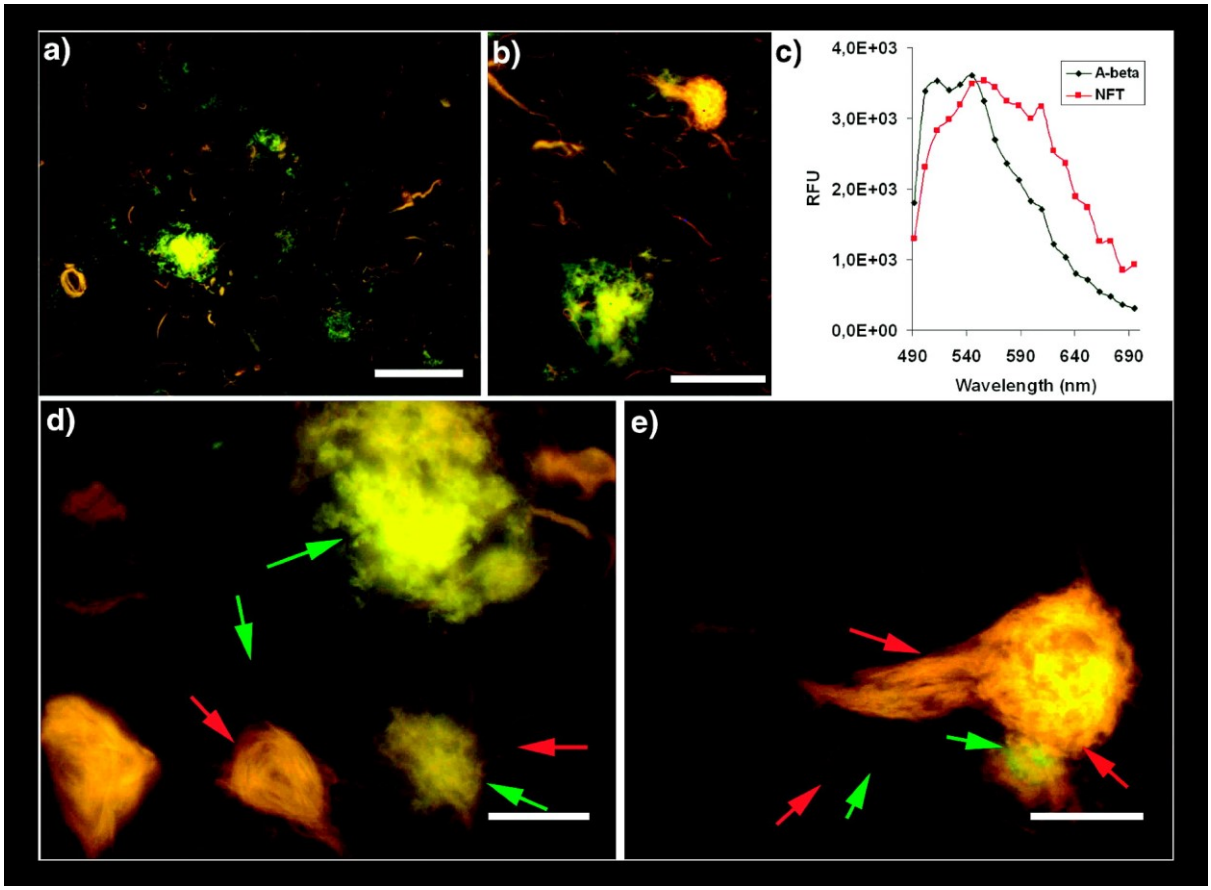


*Figure 4. High resolution fluorescence images and emission spectra of pFTAA bound to pathogenic hallmarks in AD. a,b) Fluorescence images showing an overview of the interaction between Aβ deposits (green), NFTs, and dystrophic neurites (yellow and red). c) Emission spectra of pFTAA bound to Aβ aggregates (green spectrum) or NFTs (red spectrum). d,e) High resolution fluorescence images showing the details of the distribution between Aβ deposits (green), NFTs, and dystrophic neurites (yellow and red). Selected Aβ deposits and NFTs are highlighted (green and red arrows, respectively) to indicate striking spatial co-localisation. Scale bar = 50 μm (a), 20 μm (b) and 10 μm (d and e). Figure adapted from Aslund et al. [124].*

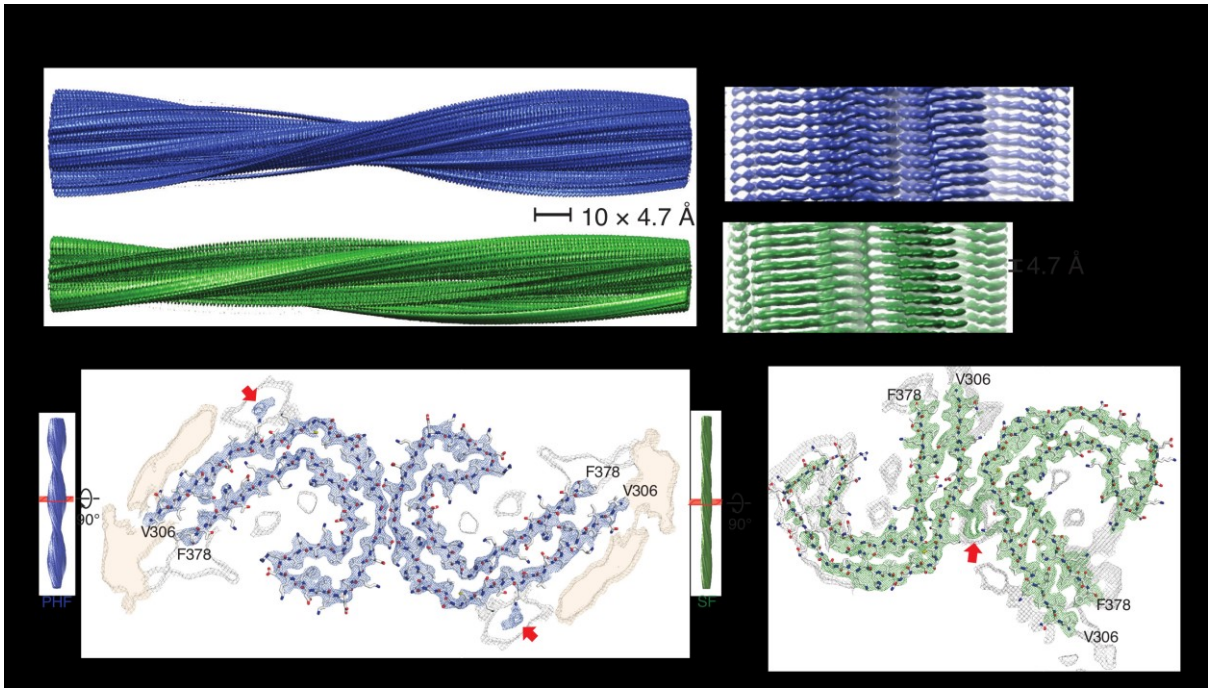


*Figure 5. AD tau filaments at atomic resolution. a,b) Cryo-EM reconstructions of PHFs (blue) and SFs (green). c,d) Cryo-EM density and atomic models of PHFs (c) and SFs (d). Overviews of the helical reconstructions (left) show the orientation of the cross-sectional densities (right). Sharpened, high-resolution maps are shown in blue (PHFs) and green (SFs). Red arrows indicate additional densities in contact with K317 and K321. Unsharpened, 4.5 Å low-pass filtered density is shown in grey. Figure adapted from Fitzpatrick et al. [78].*

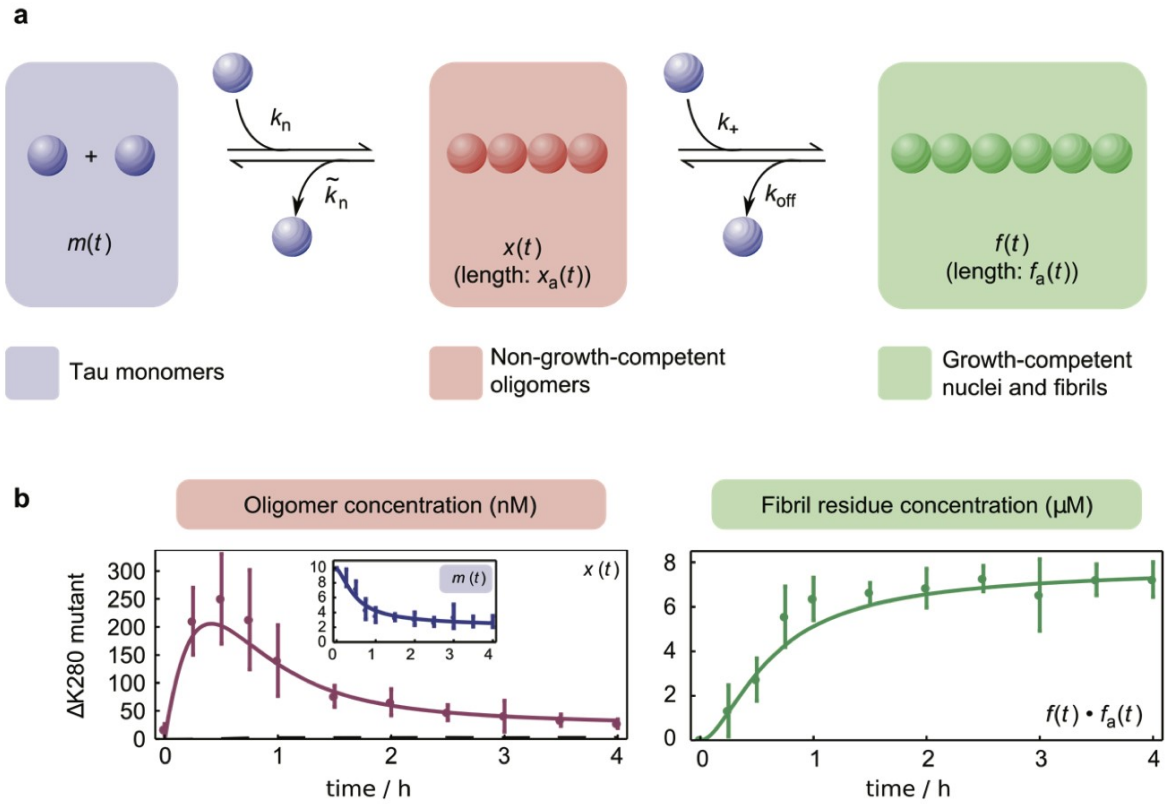


*Figure 6 Kinetic analysis of single-molecule data identifies conversion step of tau during aggregation. a) Coarse-grained on-pathway conversion model of tau oligomers. Initial formation of non-growth-competent oligomeric species x(t), of average length $x_a(t)$, occurs via a reaction of order $n_c$ in monomer concentration m(t). Formation of fibrils f(t), of average length $f_a(t)$, then proceeds via addition of monomer units in a reaction of first order in m(t). Rate constants (k) for these processes and their corresponding reverse reactions are labelled. b) Oligomeric and (deduced) fibrillar concentrations during the aggregation of K18-ΔK280 tau. Best fits for coarse-grained nucleation–conversion–polymerisation description for K18-ΔK280 are shown as solid lines. Figure adapted from Shammas et al. [165].*

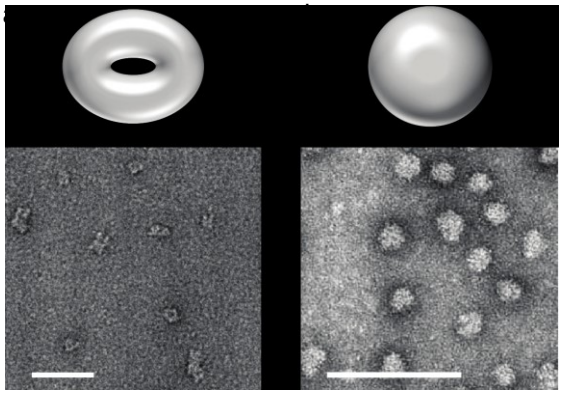

*Figure 7 TEM images of oligomers. a) Annular oligomers described for the first time by Lashuel et al. [205] formed by dissolving lyophilised αS in PBS at a concentration ranging from 300-700 μM and incubating on ice for 30-60 min. Oligomers were then filtered through 0.22 μm filters and separated from monomers by gel filtration. Scale bar is 50 nm. b) Spherical oligomers as observed by Ehrnhoefer et al. [213]. 100 μM αS was incubated in the presence of N-epigallocatechin gallate (1:10) and incubated in TBS buffer on a rotary shaker*

*(conditions favouring aggregation) at 37°C. Oligomers were separated from monomers and other aggregates by gel filtration. Scale bar is 100 nm. Adapted from Ehrnhoefer et al. [213]*

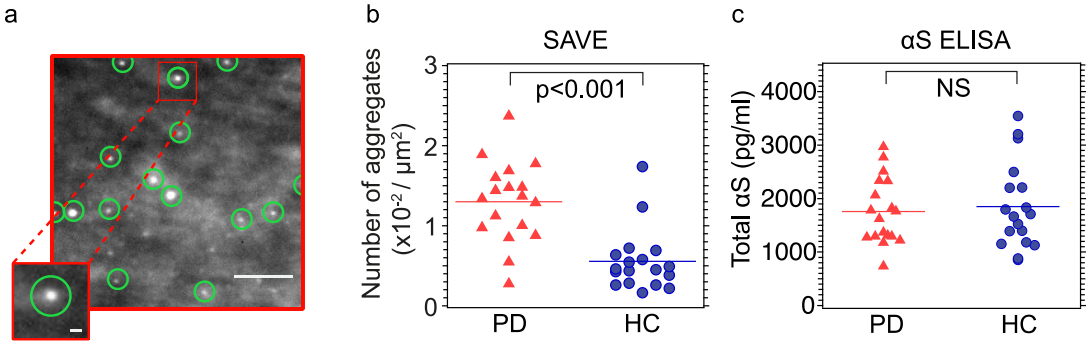


*Figure 8 SAVE imaging of αS aggregates in cerebrospinal fluid. a) SAVE image from a PD sample. Green circles show detected oligomers. Scale bar is 5 µm in the main image, and 500 nm in the zoomed inset. b) Mean number of oligomers detected for each CSF. Horizontal lines show the mean counts for PD and HC samples. c) Box plots of total αS concentrations from ELISA measurement. Even though the total αS load is not significantly different between the PD and HC samples, SAVE imaging detects significantly more aggregates in the PD samples. Figure adapted from Horrocks et al. [51].*

| Sample / Technique | fibrillar aggregates | soluble aggregates | homogeneous | heterogeneous | typical working range [mol/L] | site-specific label required | in vivo | in vitro | typical resolution |
|---|---|---|---|---|---|---|---|---|---|
| AFM | ✓ | ✓ | ✓ | ⊘ | $10^{-5}$-$10^{-7}$ | ⊘ | ⊘ | ✓ | ~1-10 nm |
| TEM | ✓ | ✓ | ✓ | ✓ | $10^{-5}$-$10^{-7}$ | ⊘ | ⊘ * | ✓ | ~1-10 nm |
| cryo-EM | ✓ | > ~100kDa | ✓ | ⊘ | $10^{-2}$-$10^{-4}$ | ⊘ | tomography | ✓ | ~0.5 nm |
| X-Ray Crystallography | ✓ | ⊘ | ✓ | ⊘ | $10^{-1}$-$10^{-3}$ crystals | ⊘ | ⊘ | ✓ | ~0.2-0.8 nm |
| NMR | ✓ | only high homogeneity | ✓ | ⊘ | $10^{-3}$-$10^{-6}$ | ⊘ # | in cell NMR | ✓ | atomic |
| SR microscopy | ✓ | ✓ | ✓ | ✓ | $10^{-6}$-$10^{-9}$ | ✓ * | ✓ | ✓ | ~20 nm |
| confocal microscopy | ✓ | ✓ | ✓ | ✓ | $10^{-9}$-$10^{-12}$ | ✓ * | ✓ | ✓ | ~250 nm |
| kinetic modelling | ✓ | ⊘ ^ | ✓ | ⊘ | $10^{-5}$-$10^{-6}$ | ⊘ | ⊘ | ✓ | ⊘ |
| ensemble methods | ✓ | ✓ | ✓ | ✓ | $10^{-3}$-$10^{-9}$ | ⊘ | some | ✓ | ⊘ |

* the use of antibodies or extrinsically fluorescent dyes allows imaging without covalently attached label
\# 13C or 1H or 14N need to be incorporated
^ mechanistic details can be inferred but soluble aggregates are not observed directly

*Table 1 Overview of possible techniques for the measurement of various aggregated proteins and their typical application spectrum. A green tick means that the indicated technique is typically viable within the given parameters of the sample whereas the red crossed circle indicates it is not. This table is by no means exhaustive and under certain circumstances measurements are still viable outside the indicated ranges and applications.*

*It should give however a quick visual aid to find the right biophysical technique for specific applications observing amyloid proteins.*